

Nottingham Castle Visitor Centre.

Geoarchaeological Borehole Monitoring



Prepared for Cal Warren / Nottingham City Council

G. Kinsley (SLR Consulting) and T.Keyworth (Trent & Peak Archaeology)

Report Number:074/2018



TPA Project Code: NCA14

Trent & Peak Archaeology ©
Unit 1, Holly Lane
Chilwell
Nottingham
NG9 4AB
0115 8967400 (Tel.)
0115 925 9464 (Fax.)
tparchaeology.co.uk
trentpeak@yorkat.co.uk



Client Name: Cal Warren / Nottingham City Council.
Document Title: Nottingham Castle Visitor Centre. Geoarchaeological Borehole Monitoring.
Document Type: FinalReport
Issue/Version Number: V2r1
Grid Reference: SK5694839561
Planning Reference: N/A
TPA Site Code: NCA14

Report No. 044/2018

Issue Number	V2r1
Prepared by	Tom Keyworth Gavin Kinsley (SLR Consulting)
Date	19/12/18
Checked by	Kristina Krawiec
Signed	
Date	19/012/18
Approved by	
Date	19/12/18
Status	V2r1

Disclaimer

This Report has been prepared solely for the person/party which commissioned it and for the specifically titled project or named part thereof referred to in the Report. The Report should not be relied upon or used for any other project by the commissioning person/party without first obtaining independent verification as to its suitability for such other project, and obtaining the prior written approval of York Archaeological Trust for Excavation and Research Limited ("YAT") (trading as Trent & Peak Archaeology) YAT accepts no responsibility or liability for the consequences of this Report being relied upon or used for any purpose other than the purpose for which it was specifically commissioned. Nobody is entitled to rely upon this Report other than the person/party which commissioned it. YAT accepts no responsibility or liability for any use of or reliance upon this Report by anybody other than the commissioning person/party.

Summary

This report sets out the archaeological context of the Visitor Centre site at Nottingham Castle where geotechnical cores were drilled on site and recorded on site in April 2018 by Trent & Peak Archaeology. It also comments on the significance of the results of the recording.

The Site lies in the castle's Outer Bailey, approximately 11m south of the medieval Outer Gate and 6m west of the Outer Bailey curtain wall. Previous fieldwork has identified the intact inner face of the medieval curtain wall and its wall-walk adjacent to the north edge of the Site, with possible medieval deposits abutting it approximately 1m below the current surface. Other work has identified near-surface medieval stratigraphy west of the Gatehouse. Medieval documentation of the Outer Bailey is sparse, possibly reflecting a low level of building there, but an earthwork rampart of the Norman period could lie within the Site. There is also the possibility of the survival of remains of later buildings.

The documentary evidence suggested that deposits relating to cultivation were to be expected dating from the 17th century onwards, which relate to the Ducal Palace. However the borehole survey recorded exclusively 19th-20th century landscaping deposits in the upper sequence which were widespread across the area with a thickness of at least 1m.

The eighteen geotechnical cores monitored indicated a deep sequence of deposits to a depth of up to 10m below ground level, with medieval artefacts lying chiefly at depths between 2.5 and 6.6m bgl. Two cores were retained for potential further analysis. A total of two samples of organic sediment were submitted for age determination from WS22 which returned a date of c.983-1154 cal AD at a depth of 5.44mbgl. In addition WS28 was submitted for OSL dating which returned age determinations of 11.3 ka BP at 4.64mbgl, 45.6 ka BP at 6.66m bgl and 138.4ks BP at 8.61mbgl.

The nature and depth of the deposits were fairly consistent across the eighteen recorded cores. The presence of a thin waterlogged organic deposit may represent in situ accumulation possibly within a feature or layer and has been shown to date to the medieval period. In addition, WS15 recorded a large piece of sandstone and WS27, 29 and 30 recorded grey sandstone, which may suggest potential for structural remains, however this is far from certain and further ground-truthing is required to establish the nature of this deposit.

The majority of the sequence was characterised by coarse sand the origins of which are difficult to determine based solely on macroscopic inspection. The OSL dating has demonstrated that these deposits accumulated in cold-climate conditions between the Last Glacial Maximum and the Younger Dryas. The environment of these periods is characterised by alpine-tundra with areas of permafrost leading to erosion and soil movement through freeze-thaw action. The deposits recorded below 4.64m are likely to have accumulated under these conditions.

Contents

Summary	iii
Contents	iv
1. Introduction	1
1.1. Background.....	1
1.2. Geology	2
2. Archaeological Context	2
2.1. Nottingham Castle	2
2.2. Immediate Context	3
2.3. Aims and objectives.....	9
3. Methodology.....	10
4. Results	11
4.1. Borehole Survey.....	11
4.2. Finds	22
4.3. Deposit Modelling	24
4.4. Sampling.....	26
5. Discussion.....	28
5.1. Summary of the deposits	28
5.2. Interpretations.....	29
5.3. Conclusions and Recommendations	31
REFERENCES	32

Figures

Figure 1. Location of the Site in relation to the medieval castle plan

Figure 2. Plan of cores, medieval masonry, surface and bedrock elevations and areas of previous work

Figure 3. South tower of the outer gate, with bedrock showing (arrowed) at the foot

Figure 4. Inner face of curtain wall recorded in 2009

Figure 5. The Outer Bailey and Site (arrowed) in the Badder and Peat map of 1744

Figure 6. Part of An East Prospect of the Castle, published 1751.

Figure 7. Depth of bedrock (Unit A)

Figure 8. Depth of red brown deposit (Unit C)

Figure 9. Deposit model cross-section A-B

Figure 10. Deposit model cross-section C-D

Figure 11. Deposit model cross-section E-F

Figure 12: Deposit model cross section G-H

Tables

Table 1. Locations, heights, total depths and simplified stratigraphy of boreholes.

Table 2. Material recovered during geoarchaeological borehole monitoring at Nottingham Castle Visitor Centre.

Table 3. Animal bone assemblage recovered from boreholes

Table 4. Summary of general deposit sequence.

Table 5. Summary of C14 dating results

Table 6. Summary of OSL dating results

1. Introduction

1.1. Background

- 1.1.1. This document provides the results of the ge archaeological investigation of deposits within the Nottingham Castle Outer Bailey, as part of stages (Stage 1) of archaeological mitigation relating to the proposed development of a new Visitor Centre. The report was commissioned and has been prepared for Cal Warren/Nottingham City Council. It has been revised in the light of comments on an earlier draft by Scott Lomax (Nottingham City Archaeologist) and staff from Historic England.
- 1.1.2. The Visitor Centre is to be located at NGR: 456958 339553 / SK 56958 39553 (the 'Site'), within the grounds of Nottingham City Council's Nottingham Castle site (Figure 1). The Site lies in the castle's Outer Bailey, the cored area occupying approximately 340m², and extending south-east from a point approximately 11m south of the medieval fabric of the Outer Bailey Gatehouse and 6m south-west of the Outer Bailey Curtain Wall (Figure 1).



Figure 1. Location of the Site in relation to elements of the medieval castle plan

- 1.1.3. A Written Scheme of Investigation (WSI) prepared by Trent & Peak Archaeology (Krawiec 2018) outlined the methodology for geoarchaeological investigation for Stage 1. This report describes the results of a geotechnical borehole survey. The WSI describes the context for the study, relevant policy and guidance, project design, wider project aims, objectives and methodologies.
- 1.1.4. Relevant extant features and the locations of previous archaeological work are shown in Figure 2. Previous archaeological work is referred to by a recording code and number (e.g. SLR-09).

1.2. Geology

- 1.2.1. The underlying geology of the area is mapped by the BGS as the Chester Formation. The deposit is gravelly and was formed 246-251 million years ago in the Triassic Period by fluvial deposition of detrital material. At the footslope of the sandstone are Head deposits representing Quaternary reworking of the sandstone higher up the slope (<http://mapapps.bgs.ac.uk/geologyofbritain/home.html>)

2. Archaeological Context

2.1. Nottingham Castle

- 2.1.1. The documentary evidence for the castle as a whole, and much of the excavated evidence up to the 1980s, have been outlined by Drage, first published in 1989 and reprinted with an index and brief notes on subsequent archaeological findings in 1999. This brief general account of the castle is based on that study (Drage 1999) together with the results of subsequent fieldwork and more recent publications and reviewer comments. It focuses on that part of the castle which is now in the City Council's ownership, with reference to finds to the north where relevant.
- 2.1.2. Stray Mesolithic worked lithics (c. 10,000 to 4000 BC) have been found in later contexts in Drage's excavations at the castle (Drage 1999, 15). In the former Northern Bailey (north of the City Council's site) around, known as Derry Mount revealed disarticulated human remains and a dagger when levelled in 1781 (as reported in Sutton 1852, 144); the Mount and the burials have been considered to be possibly Bronze Age (Dixon et al. 2006, 17) or of 17th century date (information Scott Lomax, Nottingham City Historic Environment Record, Lomax 2013, 156). Standard Hill, imprecisely located north of the current castle site, has also been postulated as of prehistoric origin with a small amount of material recovered during evaluation work in the late 1990's (Drage 1999, 15, Elliott and Kinsley 1997). Iron Age pottery has been found within the City Council site (Drage 1999, 15) and a substantial V-shaped ditch in the former Northern Bailey produced a small quantity of probable Iron Age pottery (Dixon et al. 1997, 18). There is however no firm evidence of prehistoric fortification, or of Roman activity, at the castle itself and single penannular brooch, considered by Drage to be of 6th to 7th century date (Drage 1989, 15) has later been discounted (Dixon et al. 1997, 18 and 20).
- 2.1.3. Nottingham Castle was constructed during William the Conqueror's northern campaign of 1067/8 (Marshall and Foulds 1997, 43) and remained a royal castle until its effective sale to Francis, Earl of Rutland in 1622. Due to its administrative and strategic importance the castle underwent extensive repair and modification in many stages over the centuries of royal possession (Marshall and Foulds 1997, 43-44). The castle was subsequently developed as a palatial residence of the Duke of Newcastle

from the 1670s and following damage to the Ducal Palace by fire in 1831, the current castle site and buildings were opened as a municipal museum and art gallery with gardens by the Nottingham Corporation in 1878.

- 2.1.4. The medieval castle originally comprised three main areas: the Upper Bailey (where the Ducal Palace, now the Castle Museum, stands), the Middle Bailey (now known as The Green) and the Outer Enclosure which included the current Outer Bailey and land extending 120m further north over Standard Hill. This enclosure was divided into the Northern Bailey and the Outer Bailey (to the south) in the 13th century, and the resulting Outer Bailey has itself now been reduced to land south and west of the Outer Gate by the construction of Lenton Road which leads into The Park. Probable medieval fabric - visible, excavated or inferred - is shown in Figure 1.

2.2. Immediate Context

Medieval

- 2.2.1. The features of the castle which are most relevant to this study are the Outer Gate and the Outer Bailey defences, the visible medieval parts of which lie 9m north and 6m north-east of the Site. Medieval documentation suggests that the gate and defences were located at their current positions from the start, initially built in timber, but this has not been confirmed by excavation. In 1251 AD, the Sheriff was ordered to replace the timber defences of the Outer Bailey in stone, with a gatehouse, mural towers and curtain walls. Repairs are recorded in 1289, 1290, 1357, 1360, and 1362 AD. The existing stone gatehouse and a 15m-long adjacent stretch of curtain wall which date to this period are currently visible, while further parts of the curtain wall were encased in masonry at the beginning of the 20th century (Figure 2).
- 2.2.2. The Outer Gate was in ruin by 1525, but was probably repaired during the Pilgrimage of Grace 1536. It was again in ruin at the start of the Civil War, when it was strengthened by a hornwork in front. Its present height is shown on a mid-18th-century view (Figure 6), and was probably achieved at the slighting in 1651. In the 18th and 19th centuries it was used as a porter's lodge and main entrance to the grounds of the Ducal Palace. The gatehouse reached its current form in 1908 after extensive restoration of the north and south towers and the creation of the existing north and south annexes.

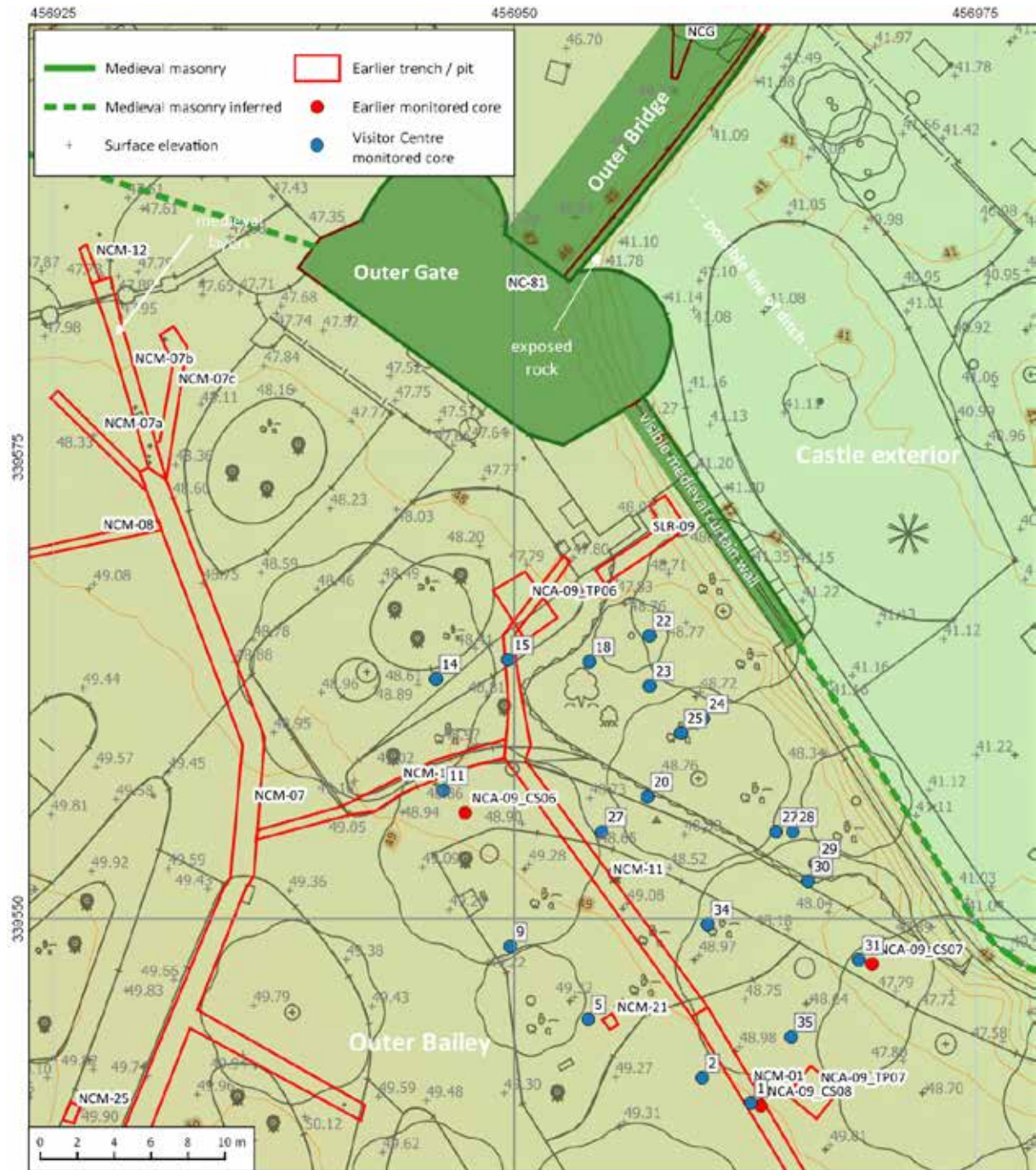


Figure 2. Plan of NCA14 cores (blue), medieval masonry (green), surface elevations and areas of previous work (red).

2.2.3. Bedrock is visible at the foot of the south tower of the Outer Gate (Figures 2 and 3). Comparison with topographical survey data suggests an elevation of at least 41.8m AOD for this rock surface. The surface levels and visible bedrock beneath the bridge in the figure convey a general impression of a wide ditched profile, but immediately south of the bridge this changes immediately to a flattened profile. This flattened area may have been formed when a Drill Hall was constructed there in 1798. The bridge arches were occupied by cottages in the 19th century and the rock beneath the inner (left hand) arch may have been excavated to form a drawbridge pit and / or later for the cottage floor.



Figure 3. South tower of the outer gate, with bedrock showing (arrowed) at the foot

- 2.2.4. The south-east tower base and the exterior face of the adjacent curtain wall have a horizontal building break at approximately 1.6m above the external ground level. In the curtain wall the face is set slightly further back above the break, and appears more weathered, but the character of the masonry is not otherwise noticeably different. The break might represent low-level patching of the wall face, or a division between different building phases. The over 7m difference in surface level from inside to outside the curtain wall might at first sight be taken to reflect a distinct change in rock level due to medieval fortification, but the levels of rock inside the Outer Bailey revealed in the coring are lower than the external ground level and it is possible that the current external levels may not have not been greatly altered since the thirteenth century, though an infilled castle defensive ditch could also be present. The lower work in the external curtain wall face may be a change in building phase, but if it is patching it is probably not of an exposed rock face (as occurs south of the Outer East Tower) but instead a re-facing of the original 13th-century wall and tower base. Drage notes that repairs to the wall were already required from the 1270s through to the early 14th century. Alternatively it is possible that the wall and tower base had originally been cut into a rampart, which when later removed exposed an unfinished masonry face which then needed re-facing.
- 2.2.5. Previous fieldwork adjacent to the north end of the Visitor Centre area (SLR-09) identified the intact inner face of the curtain wall and its wall-walk, with possible medieval deposits abutting it approximately 1m below the current surface (Figure 4, walls 16, 11 and 7) (SLR Consulting 2013). The interior face of the curtain wall at the top from the third course down and the exterior face from below the top nine courses (estimated at perhaps 1.5m) is of similar character to the outer face and it appears that this part of the curtain wall may all be the original build of the 1250s from near the parapet down to the external ground level.



Figure 4. Inner face of curtain wall recorded in 2009

- 2.2.6. Archaeological monitoring and recording of utility installations in the vicinity of the Site (NCM-07, NCM-10, NCM-11 and other NCM codes) indicated that the bulk of ground cut through by the approximately 1m deep trenches consists of post-medieval soil deposits derived from cultivation and / or landscaping. However, in the north end of trench NCM-07b medieval deposits west of the Gatehouse lay within approximately 200mm of the surface. These have been considered to indicate the surviving top of the presumed earthwork defences of the castle constructed 1067 AD.
- 2.2.7. In 2016, a programme of test pitting was carried out across the castle grounds as part of enabling works which recorded the deposits within the proposed visitor centre footprint (2016 Roushannafas and Smart). Test pits 6 (excavated to 1.50m bgl) and 7 (2.60m bgl), to the north west and south east of the footprint respectively. Test Pit 6 recorded post-medieval possible garden features which contained residual Medieval pottery. The underlying deposits comprise a compacted sandstone and sand layer which was interpreted as anthropogenic in origin rather than representing the bedrock. Test pit 7 recorded similar overlying post-medieval garden deposits which sealed possibly buried soil horizons from which Medieval and Post-Medieval artefacts were recovered.

- 2.2.8. In addition, three window samples were recorded in the same area which demonstrated thick deposits of silt sand layers to a depth of 7.40m bgl. It is not clear whether these lower deposits were anthropogenically deposited or part of a general weathering of bedrock further upslope. No finds were recovered during the borehole survey.
- 2.2.9. A 'great house and newly built houses' in the Outer Bailey were repaired in 1331-3 to accommodate the Justices in Eyre (the hall of pleas in the town being in decay), and in the 15th century it was used for grazing (Drage 1989: 12). The scarcity of medieval documentary references to work in the Outer Bailey suggests that it may have contained relatively little building, but practical considerations suggest that such building may have been close to the gatehouse and the way up to the Middle Bailey bridge, and thus potentially within the Site. Excavation in SLR-09 indicated a possible stone structure built into the inner face of the curtain wall immediately south of the Outer Gate.

Post-medieval

- 2.2.10. A plan for the very finest gardens covering 60 acres (24ha) was 'laid out' in 1724 but they were then 'not yet finished' (Defoe 1724). An area this size would have included the whole current castle grounds and the medieval Park to the west. By 1746 the Ducal Palace was described as 'much neglected' and the plan for the gardens had been abandoned in favour of a park (Simpson 1746). The Badder and Peat map of 1744, published by Deering in 1751 (Deering 1751), shows the southern part of the Outer Bailey where the Site lies occupied by small hedged and sub-divided plots containing a variety of crops. It has the appearance of a kitchen garden serving the Ducal Palace (Figure 5) and according to Deering it was (in the mid-18th century) a garden and tree-nursery (Deering 1751, 176). The Site is not visible in Kip and Knyff's Prospect of 1707 (Figure 6; Kip and Knyff 1707), but the parts of the Outer Bailey which are resemble the details in Badder and Peat and suggest that this layout was present by 1707.

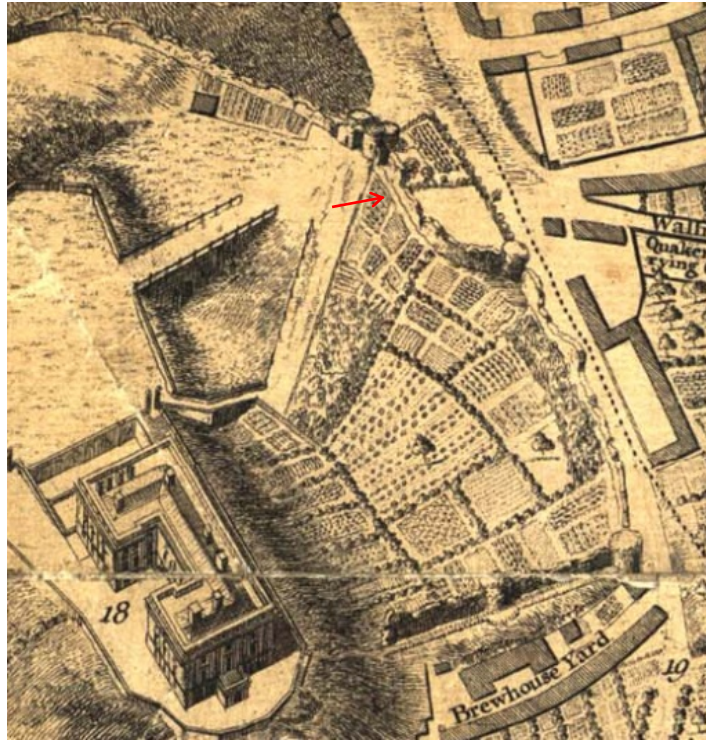


Figure 5. The Outer Bailey and Site (arrowed) in the Badder and Peat map of 1744

- 2.2.11. The location of the Site is shown arrowed in Figure 6 over An East Prospect of the Castle which is attached to the Badder and Peat map; little detail of the site itself is visible in the view. The illustration greatly reduces in appearance the true steepness of Castle Road (the road in the foreground) which climbs steeply from left to right up to the Outer Gate and is better reflected in the 1707 view.
- 2.2.12. A considerable and fairly constant height of the inner face of the curtain wall is shown in the internal view (Figure 5); notably it extends down to the base of a V-shaped notch in the masonry which is also shown from the other side in the Figure 6 view. This differs from the external view in Figure 6 which seems to show high ground close to, if not immediately behind, the inner face of the curtain wall, seen through the V-shaped notch. There is no indication of a steep downward slope approaching the inner face of the curtain wall in the Figure 6 view though other slopes are shaded.
- 2.2.13. The view shown in Figure 5 would also imply that the ground level behind the curtain wall was similar to that at the inner entrance to the gatehouse passage, which is also contrasts with the evidence of SLR-09 (Figure 4, located very close to the gatehouse) where a small volume of deposits containing only medieval pottery was excavated just below the existing ground level.
- 2.2.14. The Badder and Peat map (Figure 5) represents a slightly distorted bird's eye view based on a measured survey, and the height dimensions of the curtain wall have presumably been imagined or exaggerated, while the archaeological evidence is at present incomplete. These issues will not be resolved without further fieldwork.
- 2.2.15. Deering (1751, 176) refers to 'a low gate' built into the curtain wall between the Outer Gate and the Outer East Tower which he interpreted as a sally-port. A gate at the top of five steps is shown at this location in the East Prospect of the Castle (Figure 6, below), just to the right of the V-shaped notch but close inspection of the illustration

and comparison with the inner view suggests that the gate opens into a small hedged enclosure (shown more clearly on the plan view of the castle) outside the curtain wall. No opening is visible at this point in the inner view of the curtain wall.

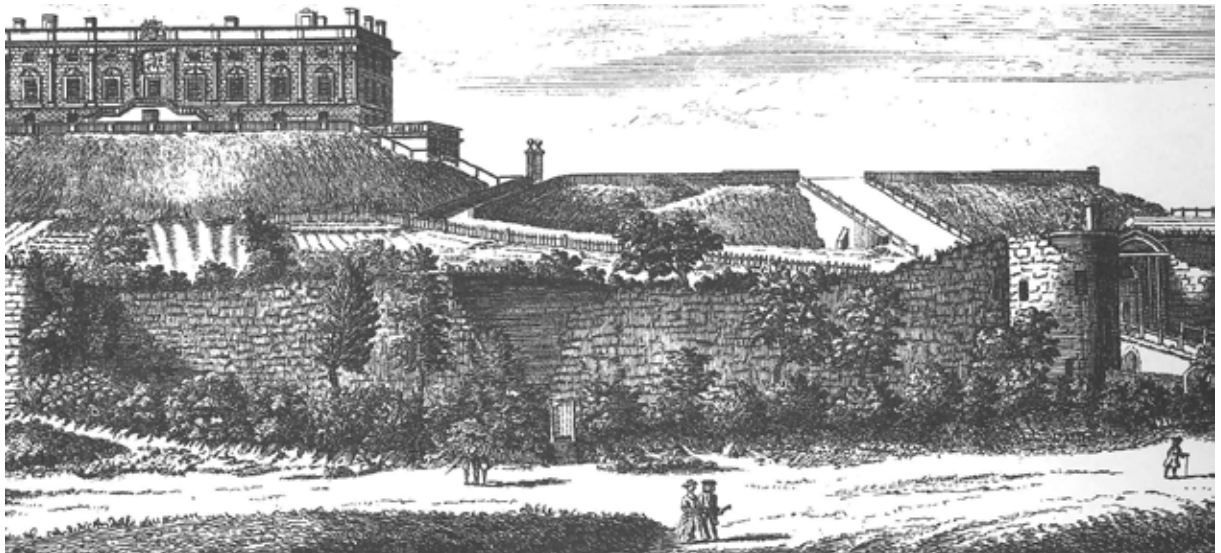
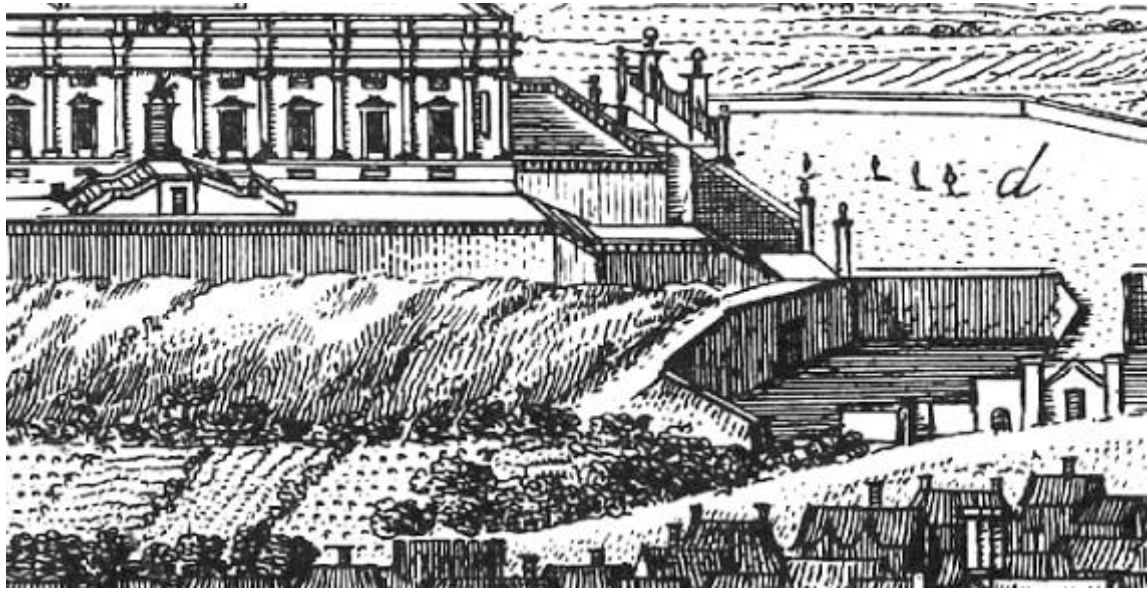


Figure 6. Part of an eastern prospect of Nottingham of 1707 (above; Kip and Kniff 1707) and of An East Prospect of the Castle, published 1751 (below; Deering 1751).

2.4. Aims and objectives

2.4.1. The aims of the borehole survey were to:

- characterise the nature, origin and development of the underlying deposits;
- characterise the palaeoenvironmental potential of the deposits and;
- refine the Stage 2 investigation strategy

2.4.2. The objectives of the survey were:

- to record the lithology of 20 boreholes;

- to create a deposit model based on the borehole logs;
- to provide a visual assessment of any retained samples for further palaeoenvironmental assessment and;
- to produce a report providing recommendations for further work.

Research questions

- 2.4.3. The project can broadly address the questions relating to the development of the pre-castle landscape. In many cases, i.e Tutbury Castle, Staffordshire and Beeston Castle Cheshire, evidence of prehistoric activity has been recorded in deposits underlying castle structures. The potential for pre-medieval human activity to exist at the castle site is high and is a research priority for the project.
- 2.4.4. More specifically the project has the potential to address the following East Midlands Research Agenda items:

7G Estates Architecture and Power:

7.4.1 High Medieval: Castle, military sites and country houses. Was there continuity of location between castles and country houses, and are earlier structures concealed in later buildings?

8.1.4 Post-Medieval: Urbanism: morphology, functions and buildings. What can studies of environmental data, artefacts and structural remains tell us about variations in diet, living conditions and status?

9.5.2 Modern: Estates, parks, gardens and woodland. What survives of country estates, parks and gardens, how are they distributed, and how should they be classified?

- 2.4.5. In addition the deeper parts of the boreholes may help to better understand the pre-castle landscape, particularly relating to possible prehistoric activity at the site.

3.5.1 Neolithic and Bronze Age: How may we characterise more effectively the frequently ephemeral structural traces that might relate to settlement activity

3. Methodology

- 3.1.1. The methodology for general fieldwork conditions was outlined in the WSI (Krawiec2018).

Borehole Survey

- 3.1.2. A total of 20 boreholes were drilled in predetermined locations representing the locations of the proposed structural piles (Figure 2). Initially, 35 locations were marked out by the structural engineer, of these only 20 were monitored as part of the original WSI. The area is part of the castle gardens with large mature trees and shrubs which prevented access to many of the locations. In total eighteen were fully recorded, with two retained for further work unopened, as per the requirements set out in the WSI (prepared with advice from NCC), and the numbering of the locations was undertaken by the structural engineer therefore the borehole numbers are often not sequential as this was carried out prior to the work being undertaken.

- 3.1.3. The boreholes were drilled using a tracked and self-propelled Windowless Sampler. The machine extracted undisturbed sediment cores in 1.00m lengths within a plastic sleeve. The sleeves were cut open on-site and the sediment lithology was recorded using standard geological nomenclature (Jones *et al.*, 1999) and in line with Historic England Guidelines for Environmental Archaeology and Geoarchaeology (Historic England 2015a and b), supplemented by colour digital photography. The boreholes were drilled until the top of the Nottingham Castle Sandstone Formation was encountered and further progress was refused.
- 3.1.4. In instances where organic material was encountered material for radiocarbon dating was retained as well as small grab samples for palaeoenvironmental assessment. A single 1.00m length of core (WS22) was retained in its entirety, as well as the entire core for WS28 (unopened to allow for possible OSL dating).

Deposit Modelling

- 3.1.5. From the recorded sediment broad lithostratigraphic units were defined.
- 3.1.6. The density of the borehole / pile locations allows for modelling of sub-surface topography and/or deposits. Utilising QGIS, two-dimensional surface models were produced using a function employing a thin plate spline algorithm. This method uses multidimensional interpolation, producing a smooth surface.
- 3.1.7. An arbitrary boundary was produced in order to constrain the area in which the model was produced and this does not reflect the proposed Visitor Centre footprint but was produced for modelling purposes only.
- 3.1.8. Two models were produced using this methodology: 1) the height AOD at which the top of the Nottingham Castle Sandstone Formation was encountered and; 2) the height AOD at which a reddish brown sandy clay deposit was observed. This allowed for: 1) the potential palaeo-landsurface to be visualised; 2) the deposits immediately overlying the sandstone bedrock to be visualised - both providing valuable information with regards to the extent of possible ground modification.

4. Results

4.1. Borehole Survey

- 4.1.1. In total, 20 boreholes were drilled within the area of the proposed Visitor Centre (Figure 2). The precise locations, heights, total depths and simplified stratigraphic units of the boreholes are summarised in the table below.
- 4.1.2. The recorded lithology is outlined below Table 1 for individual boreholes from which the broad simplified stratigraphic units are derived. The units and any associated anthropogenic finds are discussed in section 5.

Bore hole	Easting	Northing	Height (m AOD)	Total Depth (m BGL)	Simplified Stratigraphy (m BGL)
1	456962.818	339540.035	49.00	8.00	0.00-2.00 Garden Layers / Deposits 2.00-6.10 Mixed Sand Deposits 6.10-8.00 Reddish Brown Clay Deposit
2	456960.179	339541.392	48.98	10.00	0.00-2.10 Garden Layers / Deposits 2.10-6.20 Mixed Sand Deposits 6.20-8.00 Sand/Clay Deposit 8.00-8.80 Laminated Sand 8.80-10.00 Nottingham Castle Sandstone Formation
5	456954.002	339544.567	49.32	10.00	0.00-2.00 Garden Layers / Deposits 2.00-8.40 Mixed Sand Deposits 8.40-8.60 Organic Deposit 8.60-8.80 Mixed Sand Deposits 8.80-9.50 Sand/Clay Deposit 9.50-10.00 Nottingham Castle Sandstone Formation
9	456949.765	339548.516	49.22	9.00	0.00-2.70 Garden Layers / Deposits 2.70-7.00 Mixed Sand Deposits 7.00-7.50 Sand/Clay Deposit 7.50-8.50 Laminated Sand 8.50-9.00 Nottingham Castle Sandstone Formation
11	456946.125	339556.957	48.86	8.00	0.00-1.80 Garden Layers / Deposits 1.80-5.00 Mixed Sand Deposits 5.00-7.50 Sand/Clay Deposit 7.50-8.00 Nottingham Castle Sandstone Formation
14	456945.736	339563.002	48.61	8.00	0.00-1.30 Garden Layers / Deposits 1.30-3.65 Mixed Sand Deposits 3.65-3.70 Organic Deposit 3.70-6.30 Mixed Sand Deposits 6.30-7.80 Sand/Clay Deposit 7.80-8.00 Nottingham Castle Sandstone Formation
15	456949.651	339564.042	48.81	9.00	0.00-1.00 Garden Layers / Deposits 1.00-5.30 Mixed Sand Deposits 5.30-7.70 Sand/Clay Deposit with large sandstone fragment 7.70-8.70 Laminated Sand 8.70-9.00 Nottingham Castle Sandstone Formation

Bore hole	Easting	Northing	Height (m AOD)	Total Depth (m BGL)	Simplified Stratigraphy (m BGL)
18	456954.059	339563.933	48.52	10.00	0.00-2.00 Garden Layers / Deposits 2.00-5.40 Mixed Sand Deposits 5.40-5.50 Organic Deposit 5.50-5.70 Mixed Sand Deposits 5.70-6.30 Reddish Brown Clay Deposit 6.30-7.70 Mixed Gravelly Sand 7.70-8.70 Laminated Sand 8.70-10.00 Nottingham Castle Sandstone Formation
20	456957.211	339556.624	48.76	10.00	0.00-1.85 Garden Layers / Deposits 1.85-7.00 Mixed Sand Deposits 7.00-8.10 Reddish Brown Clay Deposit 8.10-9.30 Laminated Sand 9.30-10.00 Nottingham Castle Sandstone Formation
22	456957.324	339565.340	48.77	9.00	0.00-3.70 Garden Layers / Deposits 3.70-5.60 Mixed Sand Deposits 5.60-5.70 Organic Deposit 5.70-6.00 Mixed Sand Deposits 6.00-8.00 Reddish Brown Clay Deposit 8.00-8.90 Laminated Sand 8.90-9.00 Nottingham Castle Sandstone Formation
23	456957.324	339562.616	48.62	10.00	0.00-1.80 Garden Layers / Deposits 1.80-5.40 Mixed Sand Deposits 5.40-5.60 Organic Deposit 5.60-6.20 Mixed Sand Deposits 6.20-7.90 Sand/Clay Deposit 7.90-9.80 Laminated Sand 9.80-10.00 Nottingham Castle Sandstone Formation
24	456960.232	339560.842	48.64	9.00	0.00-2.00 Garden Layers / Deposits 2.00-5.50 Mixed Sand Deposits 5.50-8.10 Reddish Brown Clay Deposit 8.10-8.90 Laminated Sand 8.90-9.00 Nottingham Castle Sandstone Formation
25	456959.035	339560.068	48.65	5.00	0.00-2.00 Garden Layers / Deposits 2.00-5.00 Mixed Sand Deposits
27	456964.187	339554.724	49.08	9.00	0.00-2.30 Garden Layers / Deposits 2.30-6.40 Mixed Sand Deposits 6.40-8.30 Reddish Brown Clay Deposit 8.30-8.90 Laminated Sand

Bore hole	Easting	Northing	Height (m AOD)	Total Depth (m BGL)	Simplified Stratigraphy (m BGL)
					8.90-9.00 Nottingham Castle Sandstone Formation
28	456965.100	339554.884	48.12	10.00	Retained Core - N/A
29	456966.322	339552.995	48.10	10.00	0.00-2.40 Garden Layers / Deposits 2.40-5.80 Mixed Sand Deposits 5.80-8.30 Sand/Clay Deposit 8.30-8.90 Laminated Sand 8.90-10.00 Nottingham Castle Sandstone Formation
30	456965.919	339552.045	48.04	9.00	0.00-1.40 Garden Layers / Deposits 1.40-7.70 Mixed Sand Deposits 7.70-8.20 Sand/Clay Deposit 8.20-8.80 Laminated Sand 8.80-9.00 Nottingham Castle Sandstone Formation
31	456968.673	339547.784	47.79	10.00	0.00-2.60 Garden Layers / Deposits 2.60-6.00 Mixed Sand Deposits 6.00-8.20 Sand/Clay Deposit 8.20-9.80 Laminated Sand 9.80-10.00 Nottingham Castle Sandstone Formation
34	456960.475	339549.695	48.98	10.00	0.00-2.30 Garden Layers / Deposits 2.30-7.00 Mixed Sand Deposits 7.00-9.80 Mixed Gravelly Sand 9.80-10.00 Nottingham Castle Sandstone Formation
35	456965.005	339543.609	48.64	10.00	0.00-2.40 Garden Layers / Deposits 2.40-7.40 Mixed Sand Deposits 7.40-7.60 Organic Deposit 7.60-8.30 Sand/Clay Deposit 8.30-9.50 Laminated Sand 9.50-10.00 Nottingham Castle Sandstone Formation

Table 1. Locations, heights, total depths and simplified stratigraphy of boreholes.

WS01

- 4.1.3. Dark greyish/black brown clayey silt topsoil with modern CBM fragments (**garden/landscaping drainage layers/deposits** - 0.00-1.30m BGL), mixed light whitish/bluish grey sandstone fragments and silty sand (**garden/landscaping drainage layer/deposits** - 1.30-2.00m BGL), mixed greyish brown sands with charcoal, ceramic fragments, bone fragments, CBM, becoming lighter and more compact with depth (**mixed sand deposits** -2.00-4.30m BGL), compact orangey brown medium sand (**mixed sand deposits** – 4.30-4.70m BGL), reddish brown medium sand (**mixed sand deposits** – 4.70-4.80m BGL), lighter reddish brown

medium sand (**mixed sand deposits** – 4.80-5.70m BGL), loose, slightly yellowish brown medium sand with quartzite pebbles (**mixed sand deposits** -5.70-6.10m BGL), mixed sand – reddish brown sandy clay with quartzite pebbles (**sand/clay deposit** – 6.10-8.10m BGL).

WS02

- 4.1.4. Dark greyish/black brown dry clayey silt with modern CBM fragments and charcoal (**garden/landscaping drainage layers/deposits** – 0.00-1.30m BGL), whitish/bluish grey sandstone fragments within a silty sand matrix (**garden/landscaping drainage layers/deposits** – 1.30-2.10m BGL), dark grey silty fine sand with charcoal flecks/smears (**mixed sand deposits** – 2.10-2.50m BGL), compact orangey brown silty sand and clayey lenses with rare quartzite pebble inclusions, charcoal flecks, sandstone fragments as above (**mixed sand deposits** 2.50-4.70m BGL), reddish brown silty sand with frequent quartzite pebbles, becoming increasingly compact and clayey with depth (**mixed sand deposits** – 4.70-6.20m BGL), clear boundary to reddish brown sandy clay with frequent quartzite pebbles, increasingly sandy with depth (**sand/clay deposit** – 6.20-8.00m BGL), laminated (0.05m) and alternating yellowish grey/reddish brown fine-medium sand (**laminated sand** – 8.00-8.80m BGL), degraded yellowish grey sandstone (**Nottingham Castle Sandstone Formation** – 8.80-10.00m BGL).

WS05

- 4.1.5. Dark grey/black clayey silt with modern CBM fragments (**garden/landscaping drainage layers/deposits** 0.00-1.30m BGL), whitish light grey silty sand (fine) with sandstone fragments (**garden/landscaping drainage layer/deposits** 1.30-2.00m BGL), dark brown silty sand with frequent quartzite pebbles and charcoal fragments / flecks (**mixed sand deposits** – 2.00-2.60m BGL), change to slightly lighter orangey brown silty sand, with frequent quartzite pebbles (**mixed sand deposits** – 2.60-4.30m BGL), yellowish orangey brown sand with silt, charcoal band at 4.50-4.55m BGL, with main deposit becoming lighter/looser with depth (**mixed sand deposits** – 4.30-6.00m BGL), darker slightly orangey brown firm silty sand with clay lenses, still with charcoal fragments and rare pebbles (**mixed sand deposits** – 6.00-7.40m BGL), change to medium yellowish grey sand with dark orangey brown clayey lenses (**mixed sand deposits** – 7.40-8.40m BGL), dark greyish brown desiccated silty clay (**organic deposit** – 8.40-8.60m BGL), laminated (0.05m) sand with charcoal smears and quartzite pebbles with moderate fragments of sandstone (**mixed sand deposits** – 8.60-8.80m BGL), reddish brown clayey sand/sandy clay with rare charcoal smears (**reddish brown clayey sand** – 8.80-9.50m BGL), laminated yellowish brown sand and degraded sandstone (**Nottingham Castle Sandstone Formation** – 9.50-10.00m BGL).

WS09

- 4.1.6. Dark brown slightly clayey silt with modern CBM and glass (**garden/landscaping drainage layers/deposits** – 0.00-1.20m BGL), bluish grey sandstone within sandy silt matrix (**garden/landscaping drainage layers/deposits** – 1.20-1.50m BGL), mixed sandstone rubble/fragments within dark greyish brown sandy clay, with charcoal and CBM, becoming lighter with depth (**gardening/landscaping drainage layers/deposits** – 1.50-2.70m BGL), mixed orangey brown sand with charcoal and clay lenses (**mixed sand deposits** - 2.70-4.70m BGL), mid-dark slightly reddish brown/orangey brown sand (**mixed sand deposits** - 4.70-5.00m BGL), mixed slightly darker orangey brown sand with frequent fragments of CBM, charcoal and ceramics (**mixed sand deposits**

5.00-7.00mBGL), reddish brown sandy clay with frequent quartzite pebbles (**sand/clay deposit** – 7.00-7.50m BGL), laminated yellowish brown/orangey brown sand (**laminated sand** – 7.50-8.50m BGL), yellowish brown degraded sandstone (**Nottingham Castle Sandstone Formation** 8.50-9.00m BGL).

WS11

- 4.1.7. Dark grey/black tarmac and associated artificial gravel levelling material (**garden/landscaping drainage layers/deposits** – 0.00-0.30m BGL), mixed mid-dark greyish brown topsoil with modern ceramic, sandstone, and CBM fragments (**garden/landscaping drainage layers/deposits** – 0.30-0.70m BGL), bluish grey/brown sandstone fragments with silty sand matrix (**garden/landscaping drainage layers/deposits** – 0.70-1.20m BGL), further sandstone fragments as above with darker brown sandy clay (**garden/landscaping drainage layers/deposits** – 1.20-1.50m BGL), yellowish brown mixed sand with charcoal smears becoming dark grey/black brown clayey sand, possibly a buried soil (**mixed sand deposits** – 1.50-2.20m BGL), reddish brown clayey sand with moderate quartzite pebbles, increasing in frequency with depth (**mixed sand deposits** – 2.20-3.30m BGL), merging change to yellowish/orangey brown slightly clayey sand becoming increasingly mixed and yellow with depth (**mixed sand deposits** - 3.30-3.95m BGL), clayey brownish grey sand with charcoal and greyish yellow clay band at 4.35m BGL (**mixed sand deposits** 3.95-4.50m BGL), yellowish grey sand with rare quartzite pebbles, clayey becoming increasingly light with depth (**mixed sand deposits** – 4.50-5.00m BGL), merging change to reddish brown clayey sand / sandy clay with frequent quartzite pebbles (**sand/clay deposit** 5.00-7.50m BGL), yellow/orangey brown laminated sand (**Nottingham Castle Sandstone Formation** 7.50-8.00m BGL).

WS14

- 4.1.8. Dark grey/black brown slightly clayey silt with sand, topsoil – with modern CBM fragments and charcoal (**garden/landscaping drainage layers/deposits** – 0.00-1.10m BGL), fine-medium yellowish brown sand with moderate quartzite pebbles (**garden/landscaping drainage layers/deposits** -1.10-1.30m BGL), greyish brown slightly clayey sand with charcoal and sandstone fragments with quartzite pebbles, possible buried soil 1.40-1.75m BGL (**mixed sand deposits** – 1.30-1.75m BGL), mixed yellowish brown sand with reddish brown clayey silt, moderate quartzite pebbles and becoming increasingly darker with depth (**mixed sand deposits** – 1.75-2.75m BGL), sand becomes lighter and then orangey brown, laminated in places (**mixed sand deposits** – 2.75-3.50m BGL), light grey clayey sand with degraded sandstone fragments (**mixed sand deposits** – 3.50-3.65m BGL), greyish brown clayey sand with charcoal and possible buried soil horizon (**organic deposit**- 3.65-3.70m BGL), mixed greyish brown clayey sand with frequent sandstone fragments and quartzite pebbles, decreasing in content from 3.75m BGL (**mixed sand deposits** -3.70-4.10m BGL), mixed yellowish sand with orangey brown sand and frequent quartzite pebble inclusions (**mixed sand deposits** – 4.10-4.55m BGL), mixed reddish brown / orangey brown banded sandy clay / clayey sand with frequent quartzite pebble inclusions, wet from 5.30-5.60m BGL (**mixed sand deposits** – 4.55-6.30m BGL), firm reddish brown clayey sand, becoming stiff with depth with quartzite pebble content decreasing (**sand/clay deposit** – 6.30-7.80m BGL), orangey brown / yellowish brown sand / degraded sandstone (**Nottingham Castle Sandstone Formation** – 7.80-8.00m BGL).

WS15

- 4.1.9. Dark brown slightly clayey silt with modern CBM and glass fragments (**garden/landscaping drainage layers/deposits** – 0.00-1.00m BGL), greyish brown slightly clayey sand (**mixed sand deposits** -1.00-1.30m BGL), mixed reddish brown/orangey brown silty sand(**mixed sand deposits** – 1.30-2.00m BGL), reddish brown sand with silt and frequent quartzite pebbles (**mixed sand deposits** – 2.00-3.00m BGL), yellowish grey mixed sand with frequent quartzite pebbles, becoming increasingly dark with depth (**mixed sand deposits** – 3.00-3.80m BGL), dark grey clayey sand with charcoal, ceramics and sandstone fragments (**mixed sand deposits** - 3.80-4.40m BGL), banded yellowish grey sand with quartzite pebbles and large sandstone fragment * at 4.70m BGL (**mixed sand deposits** - 4.40-5.30m), clear change to mixed reddish brown clayey sand / sandy clay with pebbles and charcoal to at least 6.00m BGL (**sand/clay deposit** – 5.30-7.70m BGL), laminated yellowish/orangey grey sand (**laminated sand** – 7.70-8.70m BGL), yellowish grey/brown degraded sandstone (**Nottingham Castle Sandstone Formation** -8.70-9.00m BGL).

WS18

- 4.1.10. Dark brown friable clayey silt (topsoil) with rootlets, clay lense at 0.80m BGL (**garden/landscaping drainage layers/deposits** – 0.00-0.50m BGL), dark greyish brown sandy silt with modern CBM fragments (**garden/landscaping drainage layers/deposits** – 0.50-1.00m BGL), mixed sandstone fragments/rubble within a sandy silt matrix (**garden/landscaping drainage layers/deposits** – 1.00-1.40m BGL), degraded sandstone and less sandstone fragments, becoming mixed orangey/yellowish brown (**garden/landscaping drainage layers/deposits** – 1.40-2.00m BGL), fine to medium yellowish brown sand with small quartzite pebbles, becoming increasing dark with depth and compact (**mixed sand deposits** - 2.00-2.20m BGL), compact fine-medium sand in bandings/laminations, with sandstone fragments from 2.70m BGL onwards and becoming mixed with lighter hues of sand of the same colour (**mixed sand deposits** – 2.20-3.40m BGL), darker orangey/yellowish brown sand with quartzite pebbles (**mixed sand deposits** – 3.40-3.65m BGL), clear change to lighter yellowish brown sand with quartzite pebbles (**mixed sand deposits** – 3.65-4.90m BGL), merging to reddish brown / yellowish brown mixed compact sand (**mixed sand deposits** – 4.90-5.40m BGL), dark bluish grey/brown organic medium sand band (**organic deposit** – 5.40-5.50m BGL), medium to coarse orangey/yellowish brown sand (**mixed sand deposits** – 5.50-5.70m BGL), reddish brown clayey fine-medium sand with small rounded quartzite pebble inclusions (**sand/clay deposit** – 5.70-6.30m BGL), compact brownish yellow mixed sand with quartzite pebbles (**mixed gravelly sand** 6.30-7.30m BGL), reddish brown fine to medium sand with small-medium quartzite pebbles (**mixed gravelly sand** 7.30-7.70m BGL), clear change to orangey brown fine-medium sand, becoming yellowish brown and coarser with depth (**laminated sand** 7.70-8.70m BGL), crumbly/friable orangey/yellowish brown degraded sandstone(**Nottingham Castle Sandstone Formation** 8.70-10.00m BGL).

WS20

- 4.1.11. Dark greyish/black clayey silt topsoil (**garden/landscaping drainage layers/deposits** – 0.00-0.40m BGL), brick fragments/rubble (**garden/landscaping drainage layers/deposits** – 0.40-0.50m BGL), brick/CBM fragments, modern glass, ash, clinker (**garden/landscaping drainage layers/deposits** – 0.50-0.70m BGL), dark brown/black clayey silt with sand (**garden/landscaping drainage layers/deposits** - 0.70-1.00m BGL), mixed bluish grey silty clay with sandstone fragments/rubble (**garden/landscaping drainage layers/deposits** – 1.00-1.75m BGL), charcoal, ash and clinker (**garden/landscaping drainage layers/deposits** – 1.75-1.85m BGL), brown

silty sand with clay, becoming lighter with depth (**mixed sand deposits** – 1.85-2.40m BGL), yellowish brown medium sand (**mixed sand deposits** – 2.40-2.50m BGL), banded reddish brown sand and clay with frequent rounded quartzite pebbles and sandstone fragments (**mixed sand deposits** – 2.50-5.30m BGL), dark brown mixed sand (**mixed sand deposits** – 5.30-5.50m BGL), light yellowish brown fine-medium sand (**mixed sand deposits** – 5.50-6.10m BGL), fine-medium orangey brown sand with frequent quartzite pebbles (**mixed sand deposits** – 6.10-7.00m BGL), stiff reddish brown clayey sand with quartzite pebbles (**sand/clay deposit** – 7.00-8.10m BGL), yellowish brown sand with laminations (**laminated sand** – 8.10-9.30m BGL), yellowish brown degraded sandstone (**Nottingham Castle Sandstone Formation** 9.30-10.00m BGL).

WS22

- 4.1.12. Dark firm clayey silt with sand, modern CBM, ceramics and charcoal fragments (**garden/landscaping drainage layers/deposits** – 0.00-1.20m BGL), brick, likely Victorian (**garden/landscaping drainage layers/deposits** 1.20-1.30m BGL), greyish brown sandy silt with charcoal fragments and increasingly orangey with depth, sandstone fragments throughout (**garden/landscaping drainage layers/deposits** – 1.30-2.90m BGL), whitish light blue/grey sand and sandstone fragments (**garden/landscaping drainage layers/deposits** – 2.90-3.70m BGL), reddish brown sandy silt/silty (fine) sand with quartzite pebbles (**garden/landscaping drainage layers/deposits** – 3.70-5.00m BGL), RETAINED CORE 5.00-6.00m BGL (**organic deposit** at 5.60-5.70m BGL), reddish brown silty sand with mudstone fragments and quartzite pebbles (**sand/clay deposit** – 6.00-8.00m BGL), laminated fine-medium yellowish grey/white sand becoming slightly orangey with depth (**laminated sand** – 8.00-8.90m BGL), degraded yellowish brown sandstone (**Nottingham Castle Sandstone Formation** 8.90-9.00m BGL).

WS23

- 4.1.13. Dark/black brown friable clayey silt topsoil with rootlets (**garden/landscaping drainage layers/deposits** – 0.00-1.00m BGL), fragments of bluish grey sandstone fragments within a light yellowish grey matrix (**garden/landscaping drainage layers/deposits** – 1.00-1.80m BGL), compact mid greyish brown silt and fine sand with charcoal, becoming lighter with depth (**mixed sand deposits** - 1.80-2.40m BGL), lighter silty sand with quartzite pebbles (**mixed sand deposits** – 2.40-2.90m BGL), compact reddish brown silty fine sand with frequent charcoal fragments (**mixed sand deposits** – 2.90-3.30m BGL), loose mixed reddish brown/greyish yellow silty sand with charcoal and quartzite pebbles (**mixed sand deposits** – 3.30-3.80m BGL), clear change to compact slightly clayey reddish brown medium sand with charcoal, increasingly coarse with depth (**mixed sand deposits** – 3.80-5.00m BGL), reddish brown clayey sand with small quartzite pebbles (**mixed sand deposits** – 5.00-5.40m BGL), dark greyish brown sandy clay/silt underlain by a sandstone cobble (**organic deposit** – 5.40-5.60m BGL), yellowish grey silty sand with quartzite pebbles, no charcoal (**mixed sand deposit** – 5.60-6.20m BGL), orangey reddish brown clayey sand with frequent quartzite pebbles, becoming reddish brown with depth and increasingly compact, sandy clay from 7.00m BGL (**clay/sand deposit** – 6.20-7.90m BGL), laminated orangey yellowish brown fine-medium sand becoming increasingly coarse with depth and yellowish from 8.20m BGL (**laminated sand** – 7.90-9.80m BGL), yellowish brown degraded sandstone (**Nottingham Castle Sandstone Formation** - 9.80-1.00m BGL).

WS24

- 4.1.14. Dark/black grey friable clayey silt topsoil (**garden/landscaping drainage layers/deposits** – 0.00-0.80m BGL), mixed bluish grey silty clay with sandstone rubble/fragments (**garden/landscaping drainage layers/deposits** – 0.80-1.50m BGL), clinker, sandstone fragments, ash and modern glass (**garden/landscaping drainage layers/deposits** – 1.50-2.00m BGL), yellowish brown degraded sandstone fragments/sand (**mixed sand deposits** – 2.00-2.50m BGL), brownish grey sand with silt and charcoal fragments (**mixed sand deposits** – 2.50-2.90m BGL), reddish brown stiff clayey sand with rounded pebbles(**mixed sand deposits** – 2.90-3.40m BGL), lighter reddish brown with frequent pebbles (**mixed sand deposits** – 3.40-3.80m BGL), clear change to fine yellowish brown sand with frequent quartzite pebbles (**mixed sand deposits** – 3.80-4.00m BGL), orangey/red brown silty sand with moderate quartzite pebbles (**mixed sand deposits** – 4.00-5.00m BGL), yellowish brown clayey fine sand (**mixed sand deposits** – 5.00-5.30m BGL), hard sandstone cobble (**mixed sand deposits** – 5.30-5.40m BGL), dark grey silty sand (**mixed sand deposits** – 5.40-5.50m BGL), reddish brown sandy clay with frequent small rounded quartzite pebbles (**clay/sand deposit** – 5.50-6.00m BGL), reddish brown sandy clay merging to yellowish grey/brown clayey sand, becoming increasingly sandier with depth (**clay/sand deposit** – 6.00-6.90m BGL), reddish brown sandy clay with coarse orangey brown sand at 7.00-7.10m BGL (**clay/sand deposit** – 6.90-8.10m BGL), medium to coarse yellowish orangey brown fine-medium sand (**laminated sand** – 8.10-8.90m BGL), degraded yellowish brown sandstone (**Nottingham Castle Sandstone Formation** – 8.90-9.00m BGL).

WS25

- 4.1.15. Mixed dark greyish/black topsoil with modern CBM, wood fragments, ash and roots (**garden/landscaping drainage layers/deposits** – 0.00-0.55m BGL), ash/clinker (**garden/landscaping drainage layers/deposits** – 0.55-0.65m BGL), firm dark brown/black clayey silt with sand and charcoal fragments/flecks(**garden/landscaping drainage layers/deposits** – 0.65-1.20m BGL), clayey/silty sand, bluish grey and sandstone fragments (**garden/landscaping drainage layers/deposits** – 1.20-1.65m BGL), bluish grey sandstone fragments with silty clay matrix (**garden/landscaping drainage layers/deposits** – 1.65-2.00m BGL), mid-grey silty sand (**mixed sand deposits** – 2.25-2.50m BGL), yellowish grey silty sand with pebbles, no charcoal (**mixed sand deposits** – 2.50-3.10m BGL), reddish brown silty sand with frequent quartzite pebbles (**mixed sand deposits** – 3.10-3.60m BGL), reddish brown clayey sand with frequent quartzite pebbles and sandstone fragments (**mixed sand deposits** – 3.60-5.00m BGL).

WS27

- 4.1.16. Dark brown slightly clayey silt (**garden/landscaping drainage layers/deposits** – 0.00-1.30m BGL), yellowish brown sandstone fragments (**garden/landscaping drainage layers/deposits** – 1.30-2.30m BGL), compact sandy silt, greyish brown with charcoal fragments/flecks (**garden/landscaping drainage layers/deposits** 2.30-2.60m BGL), loose quartzite pebbles / cobbles within orangey grey/brown silty sand matrix (**mixed sand deposits** - 2.60-3.60m BGL), loose yellowish grey sand becoming compact sandstone from 4.00-4.40m BGL (**mixed sand deposits*** – 3.60-4.50m BGL), reddish brown sandy clay with quartzite pebbles (**mixed sand deposits** 4.50-5.20m BGL), mixed orangey yellow/greyish yellow sand with some banding (**mixed sand deposits** – 5.20-5.50m BGL), greyish brown sand with charcoal, CBM fragments and quartzite pebbles (**mixed sand deposits** – 5.50-5.80m BGL), dark yellowish brown sand becoming lighter whitish grey with depth with rare sandstone fragments (**mixed sand deposits** – 5.80-6.40m BGL), reddish brown sandy clay with frequent

quartzite pebbles (**sand/clay deposit** – 6.40-8.30m BGL), laminated yellowish brown/orangey brown sand (**laminated sand** – 8.30-8.90m BGL), degraded yellowish brown sandstone (**Nottingham Castle Sandstone Formation** – 8.90-9.00m BGL).

WS28

- 4.1.17. The entirety of the core (0.00-10.00m BGL) was retained and was unopened. The lithology will be recorded should further dating work be carried out.

WS29

- 4.1.18. Dark/black friable clayey silt with rootlets (**garden/landscaping drainage layers/deposits** – 0.00-0.80m BGL), brown greyish clayey silt and modern CBM, charcoal and sandstone fragments (**garden/landscaping drainage layers/deposits** – 0.80-1.70m BGL), clinker and sandstone fragments with ash and modern glass (**garden/landscaping drainage layers/deposits** - 1.70-1.80m BGL), degraded sandstone fragments, bluish grey, within clayey silt matrix with CBM, glass and ceramics (**garden/landscaping drainage layers/deposits** – 1.80-2.40m BGL), dark brown, becoming lighter with depth, silty sand with moderate charcoal fragments, becoming coarse with depth (**mixed sand deposits** – 2.40-3.50m BGL), slightly reddish brown silty sand, becoming firmer and clayey with depth (**mixed sand deposits** – 3.50-4.50m BGL), mixed sandstone fragments (**mixed sand deposits** – 4.50-4.60m BGL), reddish brown silty clay with sand and sandstone fragments (**mixed sand deposits*** – 4.60-4.80m BGL), slightly reddish/orangey brown silty sand with quartzite pebbles and charcoal fragments (**mixed sand deposits** – 4.80-5.50m BGL), large sandstone cobble with mixed sand and reddish brown clay (**mixed sand deposits** 5.50-5.80m BGL), laminated fine yellowish brown sand with clay lenses from 5.90m BGL and charcoal, further sandstone cobble at 7.20m BGL (**mixed sand deposits** – 5.80-7.20m BGL), reddish brown clayey/silty sand with quartzite pebbles and occasional charcoal smears/flecks, pebbles increasing in frequency with depth (**sand/clay deposit** – 7.20-8.30m BGL), clearly laminated fine sand with clayey sand (0.001m laminations) (**laminated sand** – 8.30-9.50m BGL), yellowish brown loose/degraded sandstone (**Nottingham Castle Sandstone Formation** – 9.50-10.00m BGL).

WS30

- 4.1.19. Dark grey/black dry clayey silt (**garden/landscaping drainage layers/deposits** – 0.00-0.30m BGL), mixed modern CBM, glass, ceramics, ash, charcoal within mid greyish brown sandy with silt matrix (**garden/landscaping drainage layers/deposits** - 0.30-0.95m BGL), yellowish brown sandstone fragments (**garden/landscaping drainage layers/deposits** – 0.95-1.40m BGL), brownish grey clayey sandy silt with sandstone fragments / charcoal (**garden/landscaping drainage layers/deposits** – 1.40-2.60m BGL), slightly reddish orangey brown silty sand with charcoal, becoming sandier with depth (**mixed sand deposits** – 2.60-3.70m BGL), large and relatively hard/compact yellowish grey sandstone (**mixed sand deposits*** – 3.70-4.00m BGL), reddish brown sandstone and sand with fragments of sandstone (**mixed sand deposits*** – 4.00-4.80m BGL), reddish brown sand with charcoal fragments (**mixed sand deposits** – 4.80-5.00m BGL), greyish brown sandstone fragments (**mixed sand deposits** – 5.00-5.40m BGL), coarse yellow/orangey brown sand with frequent quartzite pebbles (**mixed sand deposits** – 5.40-5.60m BGL), reddish brown clayey sand band (**mixed sand deposits** – 5.60-5.80m BGL), lighter yellowish brown sand becoming increasingly darker with depth and with an increasing in quartzite pebble quantity (**mixed sand deposits** – 5.80-7.00m BGL), reddish brown sand with quartzite

pebbles with yellowish banding / laminations (**mixed sand deposits** – 7.00-7.70m BGL), clayey reddish brown sand with frequent quartzite pebbles (**sand/clay deposit** – 7.70-8.20m BGL), yellowish/orangey brown laminated sand (**laminated sand** – 8.20-8.80m BGL), yellowish brown slightly laminated but degraded sandstone (**Nottingham Castle Sandstone Formation** – 8.80-9.00m BGL).

* These (WS15, 27, 29, 30) are the only instances in which possible structural remains may have been encountered. This will be discussed further below (section 5.1.3).

WS31

- 4.1.20. Tarmac, clinker and artificial levelling gravels (**garden/landscaping drainage layers/deposits** – 0.00-0.30m BGL), mixed sandstone rubble and further levelling materials for tarmac path (**garden/landscaping drainage layers/deposits** - 0.30-0.90m BGL), bluish grey sandstone fragments within silt and charcoal as well as clinker material (**garden/landscaping drainage layers/deposits** - 0.90-2.60m BGL), mixed reddish brown/yellowish grey sand with charcoal, slightly clayey, with quartzite pebbles (**mixed sand deposits** – 2.60-6.00m BGL), reddish brown clayey sand with quartzite pebbles (**sand/clay deposits** – 6.00-8.20m BGL), laminated orangey/yellowish brown/grey with inclusions of sandstone fragments (**laminated sand** – 8.20-9.80m BGL), greyish/yellowish brown degraded sandstone (**Nottingham Castle Sandstone Formation** - 9.80-10.00m BGL).

WS34

- 4.1.21. Dark greyish brown slightly clayey silt with sand and modern CBM, brick, charcoal (**garden/landscaping drainage layers/deposits** – 0.00-1.30m BGL), bluish grey sandstone fragments, CBM and ceramics within clayey silt matrix (**garden/landscaping drainage layers/deposits** – 1.30-2.30m BGL), greyish brown sand with silt and sandstone fragments with charcoal (**mixed sand deposits** – 2.30-3.40m BGL), lighter greyish brown sand with silt, loose and with moderate quartzite pebbles (**mixed sand deposits** – 3.40-4.10m BGL), loose yellowish brown sand with a sandstone cobble at 4.35m BGL (**mixed sand deposits** – 4.10-4.45m BGL), change to orangey/reddish yellow-brown mixed sand (**mixed sand deposits** – 4.45-5.00m BGL), greyish brown medium sand (**mixed sand deposits** – 5.00-5.60m BGL), orangey brown mixed sand with quartzite pebbles (**mixed sand deposits** – 5.60-7.00m BGL), mixed greyish brown sand with charcoal, ceramics, bone fragments to at least 9.50m BGL, becoming increasingly clayey from 8.00m-9.00m BGL (**mixed sand deposits** - 7.00-9.80m BGL). Degraded greyish/yellow brown sandstone (**Nottingham Castle Sandstone Formation** – 9.8-10.00m BGL).

WS35

- 4.1.22. Dark/black friable clayey silt with sand, modern CBM and charcoal (**garden/landscaping drainage layers/deposits** - 0.00-0.60m BGL), clinker, slag, CBM, and charcoal (**garden/landscaping drainage layers/deposits** – 0.60-0.90m BGL), stiff black sandy silt with charcoal and bone fragments (**garden/landscaping drainage layers/deposits** – 0.90-1.50m BGL), dark brown clayey silt with sandstone fragments, CBM, and charcoal (**garden/landscaping drainage layers/deposits** – 1.50-2.40m BGL), dark mixed silty clay with sand and charcoal with quartzite pebbles (**garden/landscaping drainage layers/deposits** – 2.40-3.00m BGL), mixed orangey brown silty sand with charcoal, ceramics, CBM (**mixed sand deposits** – 3.00-3.80m BGL), dark greyish brown silty sand with CBM and charcoal fragments (**mixed sand deposits** – 3.80-4.00m BGL), reddish brown silty sand with charcoal and frequent

quartzite pebbles (**mixed sand deposits** – 4.00-5.30m BGL), loose yellowish/grey mixed brown silty sand and reddish brown clay lenses (**mixed sand deposits** – 5.30-6.20m BGL), reddish grey firm mixed silty sand, absence of pebbles (**mixed sand deposits** -6.20-6.80m BGL), yellowish mixed brown silty sand and frequent quartzite pebbles (**mixed sand deposits** – 6.80-7.40m BGL), compact sand with clay and quartzite pebbles, possible fire cracked, with roots and charcoal (**mixed sand deposits** – 7.40-7.60m BGL), reddish brown stiff sandy clay with frequent sandstone fragments and quartzite pebbles and mudstone at 8.25-8.30m BGL (**sand/clay deposit**), laminated fine-medium orangey/yellow brown sand with clay lenses to 8.70m BGL (**laminated sand** – 8.30-9.50m BGL), degraded yellowish grey sandstone (**Nottingham Castle Sandstone Formation** – 9.50-10.00m BGL).

4.2. Finds

Alison Wilson and Dr Kris Poole

- 4.2.1. This report represents an assessment of the small quantity of material recovered during geoarchaeological borehole monitoring at Nottingham Castle visitor centre (Table 2). The finds consist of pottery (totalling 15 sherds/63g), ceramic building material (totalling 19/163g), animal bone (totalling 29/76g), glass (totalling 3/9g) and metal (totalling 1/4g).
- 4.2.2. With the exception of two modern earthenware plant pot body sherds, found in the upper layers of WS05 and in WS29, the pottery recovered during the borehole monitoring was of medieval date. The earliest piece was a sooted rim sherd found in WS35 which is likely to be Saxo-Norman, with the remaining pottery fragments of splashed ware, green glazed pottery and sandy wares dating to the 12th and 14th centuries. Although the pottery sherds are small fragments they are in a good state of preservation with very little wear or abrasion.
- 4.2.3. The ceramic building material, mostly roofing tile which was oxidised with a reduced core and in the case of the fragments recovered from WS35 with a green glaze, was medieval in date, with the exception of the fragments of tile and a small vitrified fragment with adhering ash slag recovered from WS29 which were post-medieval/modern.
- 4.2.4. The single metal find was a small fragment of possible medieval lead window, WS05, although identification is tentative.
- 4.2.5. In summary, the bulk of the finds are medieval in date, the earliest being a pottery fragment tentatively identified as Saxo-Norman which could date to the 11th century. The only finds belonging to later post-medieval and modern periods were recovered from WS05 and WS29, in particular the fragments of modern glass which take the assemblage into the 20th century. The finds assemblage as whole is representative of a site of medieval origin with later post-medieval/modern development.

Borehole	Unit	Weight (g)/Count	Depth m bgl	Material and description	Date
WS01	D	2g/1	2.50m	Roofing tile fragment, tentative medieval date	12th - 15th C.
WS01	D	1g/1	2.50m	Fragment of animal bone	Unknown
WS01	D	8g/1	3.40m	Roofing tile fragment, tentative medieval date	12th - 15th C.
WS02	D	2g/1	6.30m	Roofing tile fragment, tentative medieval date	12th - 15th C.
WS02	D	10g/1	6.50m	Roofing tile fragment, tentative medieval date	12th - 15th C.
WS05	F	10g/1	0.80m	Plant pot fragment, modern	18th - 20th C.

Borehole	Unit	Weight (g)/Count	Depth m bgl	Material and description	Date
WS05	E	7g/10	2.20m	Fragment of animal bone	Unknown
WS05	D	4g/1	7.50m	Strip of lead, possibly medieval window came	12th - 15th C.
WS09	D	13g/	6.40m	Roofing tile fragment, tentative medieval date	12th - 15th C.
WS09	D	25g/2	6.60m	Roofing tile fragment, tentative medieval date	12th - 15th C.
WS09	D	1g/1	6.60m	Pot body, oxidised, possibly medieval	12th - 15th C.
WS15	D	2g/1	3.90m	Pot body, sandy ware, trace of green glaze, medieval	12th - 14th C.
WS15	D	1g/1	3.90m	Fragment of animal bone	Unknown
WS18	E	7g/1	2.30m	Pot body, green glazed, oxidised with reduced core, medieval	12th - 14th C.
WS18	D	2g/1	3.30m	Fragment of animal bone	Unknown
WS18	D	15g/1	3.80m	Fragment of animal bone	Unknown
WS20	D	5g/1	3.30m	Pot body, oxidised with reduced core, medieval	12th - 14th C.
WS22	D	3g/1	2.90m	Pot body, Splashed Ware, medieval	12th - 13th C.
WS22	D	15g/1	3.70m	Pot base, green glazed, medieval	12th - 14th C.
WS25	E	10g/9	2.15m	Fragment of animal bone	Unknown
WS27	D	1g/1	5.50m	Pot body, green glazed, medieval	12th - 14th C.
WS29	F	35g/5	1.80m	Roofing tile fragments, tentative post-medieval date	18th - 20th C.
WS29	F	8g/3	1.80m	Glass, modern fragments	18th - 20th C.
WS29	F	14g/2	1.80m	Fragments of vitrified clay	18th - 20th C.
WS29	D	4g/1	2.50m	Pot body, earthenware, probable post-medieval date	17th - 20th C.
WS29	D	10g/1	4.50m	Fragment of animal bone	Unknown
WS29	D	4g/1	4.50m	Roofing tile fragment, undetermined date	Unknown
WS30	D	4g/1	3.30m	Roofing tile fragment, tentative medieval date	12th - 15th C.
WS30	D	2g/1	4.90m	Roofing tile fragment, tentative medieval date	12th - 15th C.
WS31	D	2g/1	3.50m	Pot body, green glazed, medieval	12th - 14th C.
WS34	D	3g/1	2.30m	Pot body, green glazed, medieval	12th - 14th C.
WS34	D	18g/2	7.30m	Fragments of animal bone	Unknown
WS34	C	10g/1	8.40m	Fragment of animal bone	Unknown
WS34	C	10g/3	8.45m	Pot body, oxidised, medieval	12th - 14th C.
WS34	C	1g/1	9.50m	Fragment of animal bone	Unknown
WS35	F	3g/1	1.20m	Fragment of animal bone	Unknown
WS35	D	6g/1	4.50m	Rim, possible Saxo-Norman	11th - 13th C.
WS35	D	47g/2	5.20m	Tile fragment, traces of glaze, medieval	12th - 14th C.

Table 2. Material recovered during geoarchaeological borehole monitoring at Nottingham Castle Visitor Centre.

Animal Bone

- 4.2.6. A total of 29 fragments of animal bone (76g) were recorded from 8 boreholes. Most of the animal remains are likely to be medieval in date and all of the bone was in good condition. The very small size of this assemblage precludes any interpretation of diet/economy at the site, but the condition of the bone means that any further excavation is likely to lead to further recovery of well-preserved remains which have potential to shed light on the Castle during the medieval period.
- 4.2.7. The bones recorded are detailed below, by borehole and the level below the ground surface (Table 3).

Borehole	Depth	Description
WS01	2.50m BGL	A fragment of rib from a medium-sized mammal. A small fragment of possible medieval tile came from this same depth.
WS05	2.20m BGL	Several fragments, probably from the same bone, given the fresh breaks. No dating evidence was found at this level.
WS15	3.90m BGL	An ulna from a crow/rook. Medieval pottery was recovered from the same level.
WS18	3.30m BGL	A possible rib fragment from a large-sized mammal. No dating evidence was recovered from this level, but medieval pottery was retrieved from 2.30m.
WS18	3.80m BGL	An atlas vertebra from a sheep/goat, with evidence of dog gnawing. No dating evidence was recovered from this level, but medieval pottery was retrieved from 2.30m.
WS25	2.15m BGL	A large mammal-sized rib, which has broken into several fragments along fresh breaks. No dating evidence was retrieved from this borehole.
WS29	4.50m BGL	A cattle calcaenus from a young animal, given its size, porous nature and unfused proximal end (indicating an age of less than 36 months old at death). No dating evidence was retrieved from this layer, but post-medieval finds were retrieved from 2.5m and above.
WS34	7.30m BGL	Two bone fragments (including one fragment that had split into two pieces along a fresh break), likely to be come from the same bone, a cattle ulna. This had been chopped through, presumably when dividing up the carcass. No dating evidence was recovered from this feature, but medieval pottery was retrieved from 2.30m and 8.45m.
WS34	8.40mBGL	Fragment of large mammal-sized long bone, with evidence of dog gnawing. Medieval pottery was found at 8.45m.
WS34	9.50mBGL	A fragment of large mammal-sized long bone.
WS35	1.20mBGL	A fragment of large mammal-sized rib. No dating evidence was found in this layer and although medieval finds were retrieved from 4.50 and 5.20m below the surface, the location of this find may suggest a post-medieval to modern date.

Table 3. Animal bone assemblage recovered from boreholes

4.3. Deposit Modelling

- 4.3.1. The lithological and stratigraphical data recorded at the site was used to construct a basic deposit model of the site. From the recorded sediment broad units were defined.
- 4.3.2. The density of the borehole / pile locations allows for modelling of sub-surface topography and/or deposits. Utilising QGIS, two-dimensional surface models were produced using a function employing a thin plate spline algorithm. This method uses multidimensional interpolation, producing a smooth surface.
- 4.3.3. An arbitrary boundary was produced in order to constrain the area of the model and this does not reflect the proposed Visitor Centre footprint but was produced for

modelling purposes only. In addition, the predetermined locations of the boreholes influenced the modelling process and this will be considered in the interpretation.

- 4.3.4. Two models were produced using this methodology: 1) the height AOD at which the top of the Nottingham Castle Sandstone Formation was encountered (Figure 7; see 4.3) and; 2) the height AOD at which a reddish brown sandy/clay deposit was observed (Figure 8; see 4.3). This allowed for the potential palaeo-landsurface to be visualised and the deposits immediately overlying the sandstone bedrock to be visualised - both providing valuable information with regards to the extent of possible ground modification.

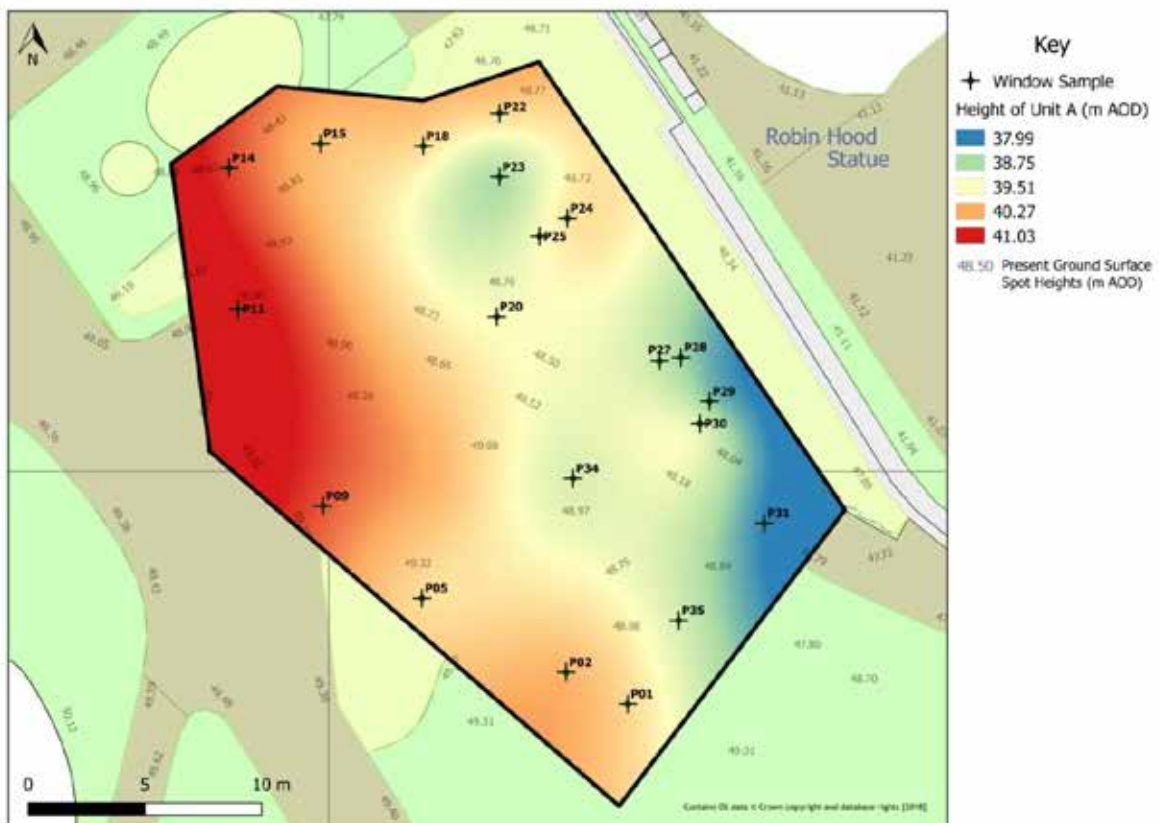


Figure 7. Depth of bedrock (Unit A)

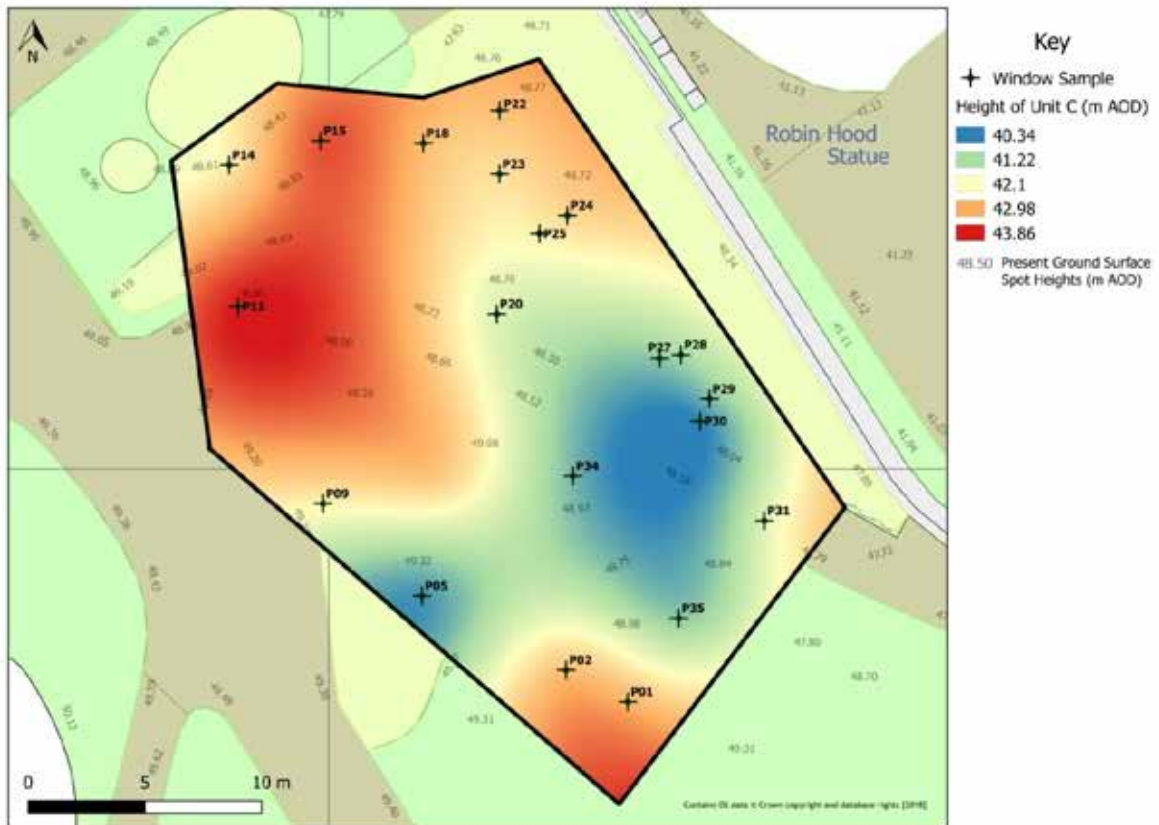


Figure 8. Depth of red brown deposit (Unit C)

Cross-Sections

- 4.3.5. The broad stratigraphic units were modelled to produce three cross-section diagrams in RockWorks: A-B (Figure 9), C-D (Figure 10), and E-F (Figure 11) – see 4.3.
- 4.3.6. This allowed for general trends within the main stratigraphic sequence to be visualised. The distribution of the boreholes largely determined the location of usable cross-section transects. The location of any organic sediments/deposits that were observed are also plotted on the individual logs within the cross-sections.

4.4. Sampling and dating

- 4.4.1. A complete and intact 10.00m core (WS28) was retained for further work as well as a 1.00m section of core from WS22. Two subsamples of the organic sediment were retained from both WS22 (5.60m bgl) and WS28 (core not opened, but presumed to be c. 5.60m). The whole core of WS28 will remain unopened to allow the deposits to be viable for OSL dating.

C14 Dating

- 4.4.2. A sample taken from WS22 at a depth of 5.44-5.46m BGL was submitted to Beta Analytic for radiocarbon dating of the humic and humin fraction of the sediment (C14). The results are summarised in the table below (see Appendix for full report):

Site code	TPA Dating No.	Dating Lab	Lab Sample Number	Window Sample	Depth range (m BGL)	Sample Type	Radiocarbon Age BP	Calibrated Date 95.4%
NCA14	TPA_023	BETA	500324	WS22	5.44-5.46	Bulk sediment humic	980 ± 30BP	1070 to 1154 cal AD (49.4%) and 993 to 1058 cal AD (46%)
NCA14	TPA_024	BETA	500325	WS22	5.44-5.46	Bulk sediment humin	1000 ± 30BP	983 to 1051 (71%), 1082 to 1128 (19.2%) and 1135 to 1152 (5.2%) cal AD

Table 5. Summary of C14 dating results

- 4.4.3. The first sample, TPA_023, returned a date of 1070-1154 and 993-1058 cal AD. The second sample, TPA_024, produced a date of 983-1051, 1082-1128, and 1135-1152 AD. This gives a possible range within the 10th-12th century or late Early Medieval to early High Medieval which in turn correlates to the period in which the castle was first established.

OSL Dating

- 4.4.4. A total of three samples were taken from WS28 at depths of 4.64, 6.66, and 8.61m BGL and submitted to the Luminescence dating laboratory at the University of Gloucestershire (Figure 12). The results are summarised in the table below (see Appendix for full report):

Field Code	Lab Code	Depth (m BGL)	Total D _r (Gy.ka ⁻¹)	D _e (Gy)	Age (ka) BP
NCA14 - WS28: 4-5 m	GL18006	4.64	2.29 ± 0.15	25.9 ± 2.5	11.3 ± 1.3 (1.2)
NCA14 - WS28: 6-7 m	GL18007	6.66	2.51 ± 0.16	114.6 ± 13.0	45.6 ± 5.9 (5.5)
NCA14 - WS28: 8-9 m	GL18008	8.61	2.79 ± 0.19	385.8 ± 40.8	138.4 ± 17.4 (15.6)

Table 6. Summary of OSL dating results

- 4.4.5. The first sample, GL18006, was taken from a depth of 4.64m BGL and produced an age of 11.3 ± 1.3ka BP. The second sample, GL18007, was taken from a depth of 6.66m BGL and produced an age of 45.6 ± 5.9ka BP. The final sample, GL18008, was taken from a depth of 8.61m BGL and produced an age of 138.4 ± 17.4ka BP.
- 4.4.6. The first two samples produced dates that have accepted age estimates (blue) whilst the third sample produced an age that may have been influenced by contamination (red) and therefore should be treated as a minimum age estimate.

5. Discussion

5.1. Summary of the deposits

- 5.1.1. The general depositional sequence indicated by the monitored cores is summarised in Table 3, with potential Units labelled upwards from A to F.
- 5.1.2. The bedrock was extremely soft and often hard to distinguish from the overlying layers (Unit A). This was encountered at between 8-10mbgl across the site. The OSL age determination returned a date of 138.4 ± 17.4 ka BP at 8.61mbgl from WS28 which indicates feldspar contamination and is therefore accepted as a minimum age estimate. At this depth the material is likely to be soft bedrock rather than colluvially-derived deposits.
- 5.1.3. The bedrock was overlain by a series of laminated sand deposits which are interpreted as possibly colluvially derived, perhaps as a result of upslope weathering of unvegetated sandstone (Unit B). The OSL age determination of 45.6ka BP, recovered from 6.66m bgl from WS28, suggesting these deposits accumulated just prior to the Last Glacial Maximum (Figure 12). The sandstone is likely to have been weathered and transported under freeze-thaw conditions
- 5.1.4. This was overlain by a deposit with a clay component with occasional quartzite pebbles again perhaps suggesting deposition via hillslope solifluction processes (Unit C). This deposit may also suggest that surface water run-off was a main factor for the movement of deposits as evidenced by the presence of clay within the sequence. The upper part of this deposit was subject to OSL dating at 4.64m bgl suggesting accumulation at the end of the Younger dryas (11.3ka BP). Again this period marks a climatic downturn and a return to peri-glacial conditions with freeze-thaw action eroding deposits further upslope. These deposits likely formed in an alpine-tundra environment with little vegetation to provide stabilisation to the soils. It is also of note that dark red sand has been used in the bedding and foundations of medieval masonry at the castle.
- 5.1.5. This unit was overlain in all cores by a more mixed silt sand deposit with frequent charcoal and sandstone fragments (Unit D). The sandstone fragments were particularly large and compact in WS15, 27, 29 and 30, which may suggest the presence of possible structural remains. It is from this unit that artefacts, including animal bone, pottery and roof tile, were recovered which date to the medieval period. This cultural material was recovered from 2.30-3.30mbgl, with a higher concentration between 3.3-6.6m bgl. In addition, an organic deposit was recorded which may suggest the presence of either discrete features or layers. This deposit is unexpected given the free-draining nature of the site and has a high palaeoenvironmental potential. This unit is most likely to represent anthropogenic deposition either as layers for landscaping or as discrete features which are unable to be distinguished in the boreholes with certainty. The radiocarbon age determinations have demonstrated that, in the location of WS22, this deposit dates to the earliest phase of the castle, (BETA-500324: 1070 to 1154 cal AD and 993 to 1058 cal AD, BETA-500325 983 to 1051, 1082 to 1128 and 1135 to 1152 cal AD).
- 5.1.6. The upper deposits are characterised by a series of rubble dominated deposits related to post-medieval and modern garden landscaping (Units E and F). These comprise the

upper 2.50m of the sequence. These are likely related to the Ducal palace and later modern garden formation. These deposits were encountered during the 2016 test pit investigations which were unable to be excavated to the potential Medieval deposits beyond 2.30mbgl (Roushannafas 2016). In addition a programme of boreholes (CS7, 8 and 9 in the vicinity of the visitor centre) was carried out which identified similar deposits to those recorded by this current study. However, these data points have not been included in the model due to the close proximity to the boreholes carried out in this phase.

Unit	Depth below ground level (BGL)	Nature of deposits	Artefacts / cultural material	Age determination
F	0.0 to ~1.85m	Made ground of gravel, clinker and topsoil	Modern material and artefacts	
E	~1.85 to ~2.50m	Sandstone fragments / rubble	Modern and post-medieval material and artefacts	
D	~2.50 to ~5.00-7.50m	Brown, grey, yellowish-brown and orangey-brown (reddish-brown with depth) silty sands with clay lenses, frequent charcoal, large sandstone fragments / cobbles, quartzite pebbles / cobbles possible structures Intermittent dark greyish-brown clayey sand with organic content between ~3.65m and 5.60m BGL (possible buried soil or surface or infilling of archaeological features)	~2.3m to 8.45m, chiefly ~3.3 to 6.6m BGL, medieval artefacts	5.44-5.46m bgl BETA-500324 1070 to 1154 cal AD (49.4%) and 993 to 1058 cal AD (46%) BETA-500325 983 to 1051, 1082 to 1128 and 1135 to 1152 cal AD
C	~5.00-7.5m to ~6.9-9.5m	Reddish-brown clayey sand / sandy clay with mudstone, quartzite pebbles	Flecks and smears of charcoal	4.64mbgl 11.3ka BP 6.66mbgl 45.6ka BP
B	~7.6-9.5m	Laminated yellowish / orangey-brown medium-fine sand with occasional reddish-brown clayey sand laminations (colluvium or weathered bedrock)		
A	~8.2-10.0m	Bedrock		8.61mbgl 138.4 ± 17.4ka BP

Table 4. Summary of general deposit sequence.

5.2. Interpretations

Bedrock Levels

- 5.2.1. The combined evidence of the above records shows that bedrock (Unit A) levels are variable but there is a hint of rising bedrock levels towards the west and north-west within the monitored area (also reflected in the overlying stratigraphy). To the west this is consistent with the general levels within the castle site. To the north the impression is supported by the presence of shallow medieval deposits west of the Outer Gate in NCA-11 and SLR-09 and the higher level of rock (even though truncated) exposed at the bridge footings. To either side of the curtain wall the low level of rock, combined with the rising surface further east on Castle Road (Figure 3), hints at a localised original natural depression lying within the Site and outside the castle south of the gatehouse and bridge. Such a depression would be a natural trap for the accumulation of colluvium.
- 5.2.2. The deposits overlying the bedrock have been demonstrated to have accumulated during cold-climate conditions. This suggests that the medieval deposits directly overlie peri-glacially weathered sediments. The possibility for deeply buried prehistoric remains to be preserved at the site is still uncertain. The potential for cut archaeological features remains high and may be preserved at variable levels across the area. The age determinations recorded from the site have demonstrated the difficulty in understanding the origin of the sediments at the site from visual observation alone. The lack of a distinct difference between the medieval deposits and the weathered sandstone makes interpretation of the deposits problematic without further study.
- 5.2.3. A natural profile formed on the sandstone would be expected to contain an approximately 1m thickness of sandstone weathered into sand, often containing laminations. Unit B could fit into this category. That would however conflict with Drage's observation of the rampart at the northern end of the Middle Bailey, which was laid directly onto cleared bedrock (see following sub-section).

Earthwork defences

- 5.2.4. The exact course and level of the earlier earthwork defences, which are thought to have existed in this vicinity, remains uncertain. The medieval documentation states that the Outer Gate, and therefore the stone curtain wall at least in the immediate vicinity, were to be built on the same line as the earthwork defences, but how exactly this was meant or carried out is uncertain. It is however quite possible that the original earthen rampart of the early castle defences lies at the back of the current curtain wall.
- 5.2.5. Excavation of the Middle Bailey rampart suggests that it was constructed on the inner face of the ditch with a dump construction and a width of perhaps 18m. It was placed on the bedrock surface from which topsoil had previously been removed (Drage 1989: 81-82). While an 11th Century date for this rampart is presumed, it is not proven. It is likely that the Outer Bailey earthwork defences were broadly contemporary with it.
- 5.2.6. An 18m-wide rampart measured back from the front face of the existing curtain wall would extend over most of the Site. The lower deposits sampled in the cores may thus include 11th Century rampart material at the base of the medieval sequence. This could be equated with Unit D as the dating from the organic deposit is consistent with the earliest phase of castle construction/use.
- 5.2.7. However, it is difficult to assess the exact nature and extent of the organic deposit observed intermittently across the site. It may represent a buried ground surface or soil but it could equally represent the infilling of an archaeological feature. The further

work carried out has demonstrated that waterlogged medieval deposits survive at the site. The artefacts recovered from the deposits are also consistent within in situ medieval activity. The animal bone assemblage is primarily food waste with evidence of secondary damage represented by canine gnaw marks.

Later medieval made ground

- 5.2.8. The middle and upper part of Unit D could represent medieval landscaping, possibly connected with buildings. This level is where most of the medieval artefacts were found. The SLR-09 work identified a possible stone wall abutting the inside face of the curtain wall 6m to the north of the Site. Buildings are known to have been present somewhere in the Outer Bailey in the 14th century and excavation identified a possible wall built into the inner face of the curtain wall just south of the outer gate (see 2.2.1).
- 5.2.9. In WS30 reddish brown sandstone and sand with fragments of sandstone was observed, above which was relatively hard/compact yellowish grey sandstone between 3.70-4.80m BGL. The location of this, some 8.00m south-west from the current Curtain Wall, leaves open the possibility of structural remains being the interpretation for this but this cannot be stated definitely. In addition, similar deposits were observed at similar depths 4.00-4.40m and 5.5-5.80m BGL in WS27 and 29 respectively. The large fragment of sandstone recorded in WS15 may also suggest a possible structural component to this deposit. The small amount of roof tile recovered from these cores may also lend weight to the presence of structures although roof tile was also recovered from cores that did not demonstrate the presence of large sandstone fragments.

Post-medieval and recent made ground

- 5.2.10. There is little to distinguish these two Units (E and F) chronologically within the depositional sequence. The post-medieval landscaping has been investigated in an extensive excavation (WDC-01 to WDC-03) 50m to the south-east of the Site, and this work provides an indication of what these Units might represent. The results are not directly comparable, but a 1m thickness of 20th century made ground overlay 19th century garden soil, and below that 'garden features' of 17th to 19th-century date consisting of vertical-sided and flat-bottomed trenches cut into a 'clean' substratum. Such trenches would be in keeping with cultivation rather than landscaping and are consistent with the layout indicated by historic mapping from at least 1707 through to the late 19th century.

5.3. Conclusions and Recommendations

- 5.3.1. The results of the borehole monitoring have demonstrated the presence of anthropogenically derived deposits to at least a depth of 7.50mbgl. The lowest deposits in the sequence overlying the bedrock have been shown to have accumulated under cold-climate conditions from the Last Glacial Maximum to the Younger Dryas. The site has also demonstrated the presence of in situ waterlogged medieval deposits dating to the earliest phase of castle use/construction. These deposits should be targeted for further sampling. The deposits within the retained cores could be subject to microfossil assessment in order to determine the origin of the deposit.

- 5.3.2. The boreholes also recorded several obstructions which may relate to structural remains, 3.7-4.80m and 4-4.40mbgl. These locations (WS15, 27, 29 and 30) would have to be clarified through open area excavation to determine nature of these obstructions. A small quantity of roof tile was also recovered which may lend weight to the possibility of either in situ structural remains or demolition events.
- 5.3.3. The retained cores have the potential to begin to address the aims presented in the WSI and the East Midlands Research questions relating to the pre-Castle landscape and the continuity of land-use. The age determinations have demonstrated that significant weathering of the bedrock has taken place under peri-glacial conditions and that the medieval deposits are likely to directly overlie these weathered deposits.

6. REFERENCES

- Deering, C. 1751. *Nottinghamia Vetus et Nova*. George Ayscough and Thomas Willington
- Defoe, D. 1724. *A tour Through the Whole Island of Great Britain*. <http://www.visionofbritain.org.uk/travellers/Defoe/29>
- Dixon, P, Knight, D and Firman R. I. 2006. 'The Origins of Nottingham', pp9-23, in Beckett, J. (ed.) *A Centenary History of Nottingham*. Manchester University Press: Manchester and New York.
- Drage, C, 1989. Nottingham Castle: A Place Full Royal. *Transactions of the Thoroton Society of Nottinghamshire 93*.
- Elliott, L and Kinsley, G. 1997. *Nottingham General Hospital, Standard Hill: A report on the archaeological evaluations December 1996-January 1997. Trent & Peak Archaeology unpublished report*.
- Kip, I., and Knyff, L. 1707. *The Prospect of Nottingham from ye East*.
- Krawiec, K. 2018. *Nottingham Castle Visitor Centre: Geoarchaeological Borehole Monitoring – Written Scheme of Investigation*. TPA Report: 045/2018.
- Lomax, S. 2013. *Nottingham: The Buried Past of a Historic City Revealed*. Pen and Sword Books Ltd.
- Marshall, P. and Foulds, T. 1997. 'The Royal Castle' in Beckett, J. (ed.) *A Centenary History of Nottingham*. Manchester University Press: Manchester and New York.
- Parker, R. and Binns, L. 2017. *We Dig the Castle! - A Community and Training Excavation in the Outer Bailey of Nottingham Castle - Interim Report for the 2015-2017 Excavations. Trent & Peak Archaeology unpublished report*.
- Roushannafas, T and Smart, K. 2016. *Nottingham Castle Redevelopment Project Archaeological Mitigation for Enabling Groundworks. Trent & Peak Archaeology unpublished report*.
- SLR Consulting. 2013. *Nottingham Castle Gatehouse Toilet Alterations: Archaeological Excavation Report and Archive* (SLR ref. 403.2929.00001).

Simpson, S. 1746. *The Agreeable Historian or the compleat English Traveller*. R Walker: Fleet Lane London 1746.

Sutton, J. 1852. *The Date-Book of Remarkable and Memorable Events connected with Nottingham and its Neighbourhood 1750-1850*. ReInk Books reprinted 2018.

Young, C, 1982. *Discovering Rescue Archaeology in Nottingham*. Nottingham City Museums.

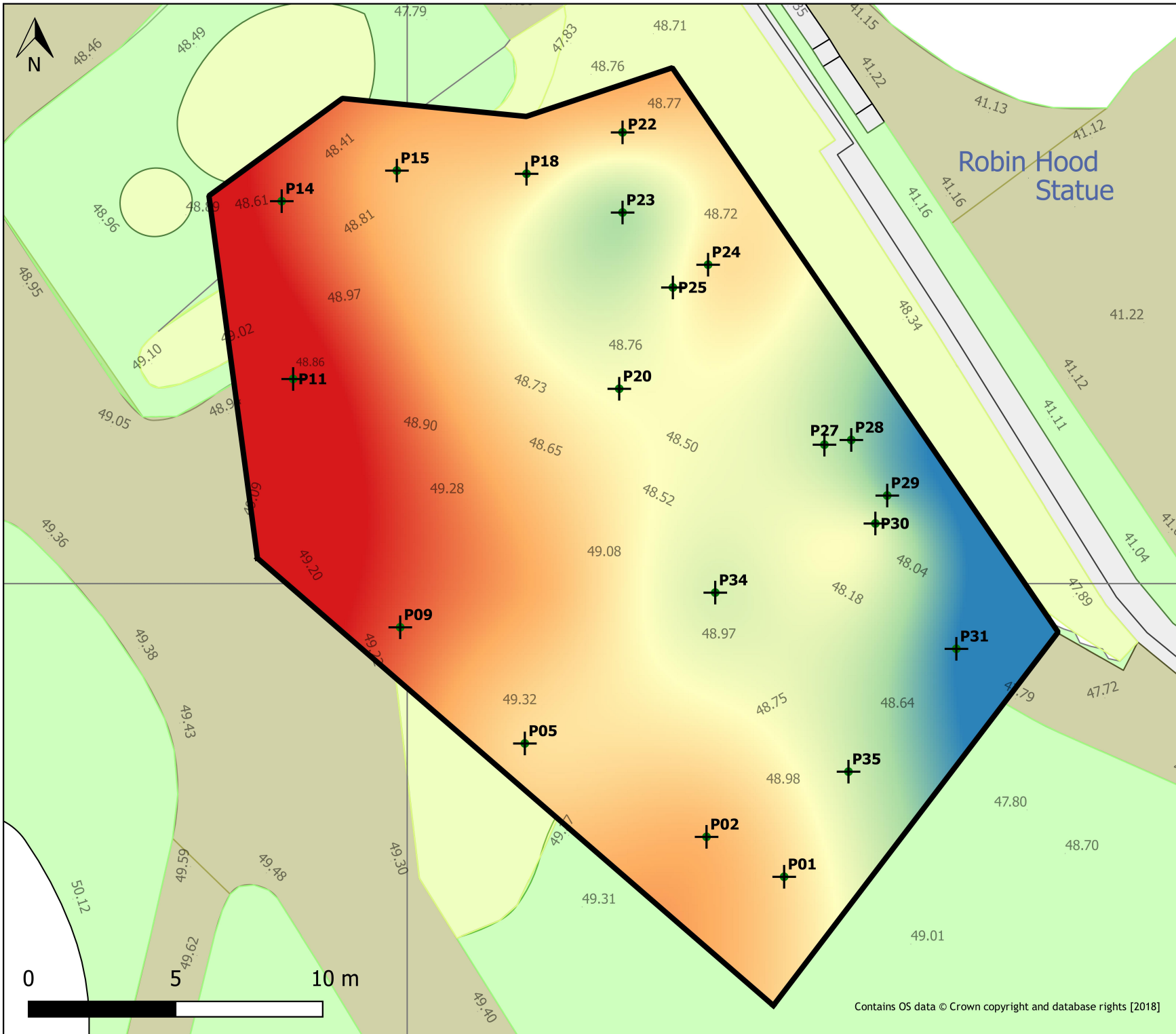
Maps

East Midlands Special Collection Not 3.B8.D44: Map of Nottingham by Badder and Peat, 1744, reproduced in C. Deering's *Historical Account of the ancient and present State of the Town of Nottingham* (1751).

<https://www.nottingham.ac.uk/manuscriptsandspecialcollections/images-multimedia/elearning/healthhousing/housing/maps/05-0504m-full.jpg>

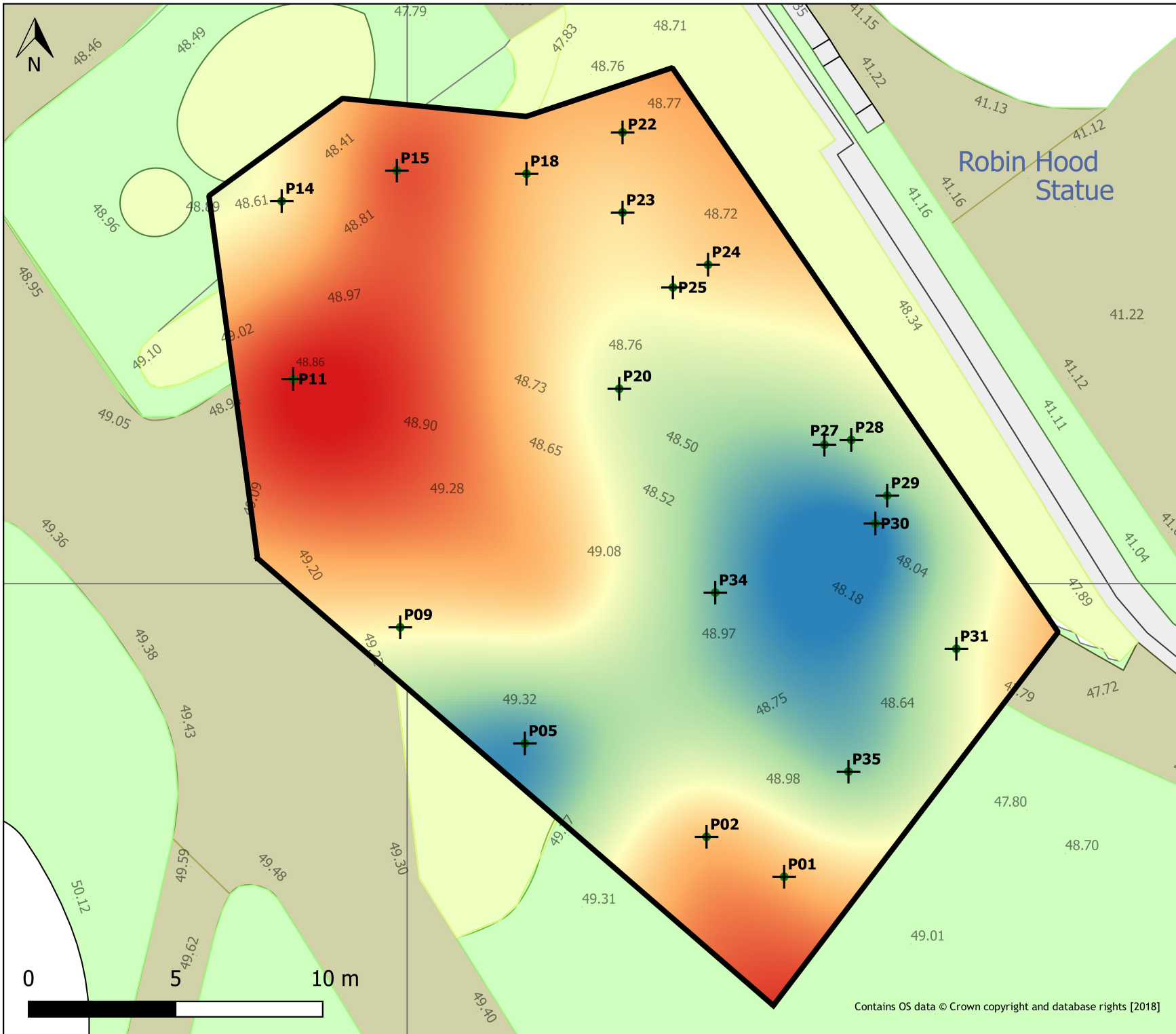
Kip, I., and Knyff, L. 1707. *The Prospect of Nottingham from ye East*.

<https://www.nottingham.ac.uk/manuscriptsandspecialcollections/images-multimedia/elearning/healthhousing/housing/maps/05-0507m-full.jpg>



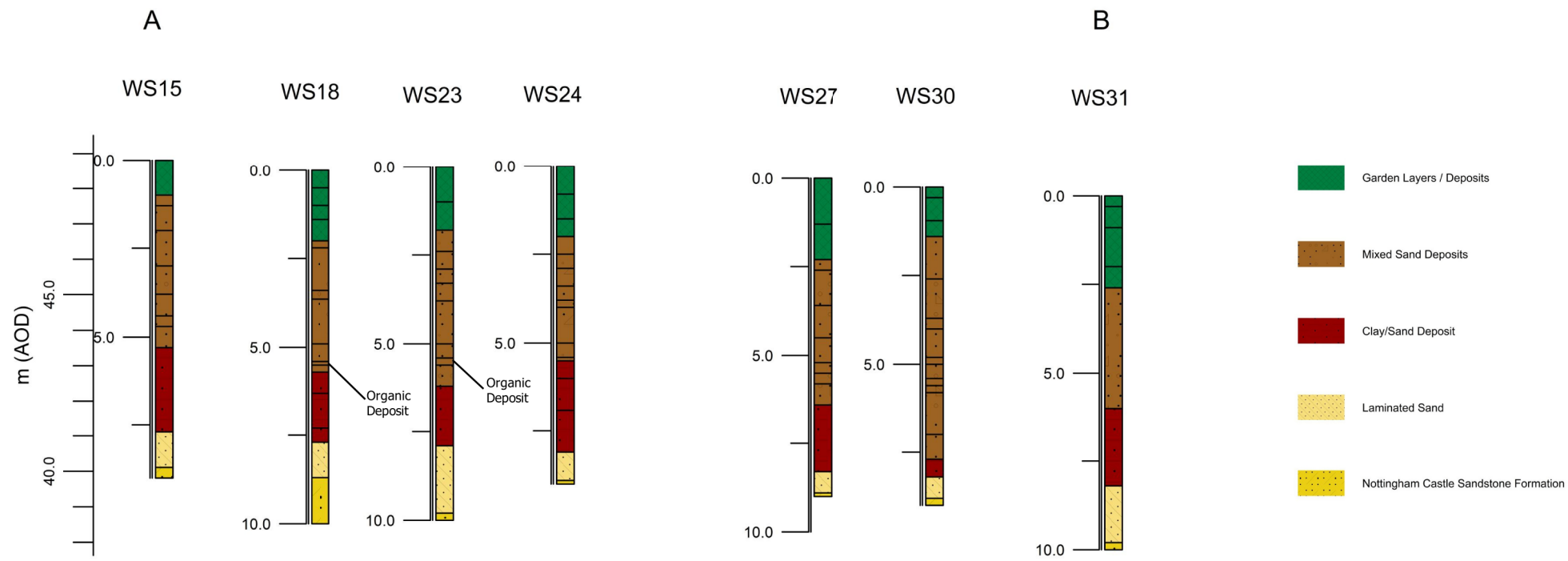
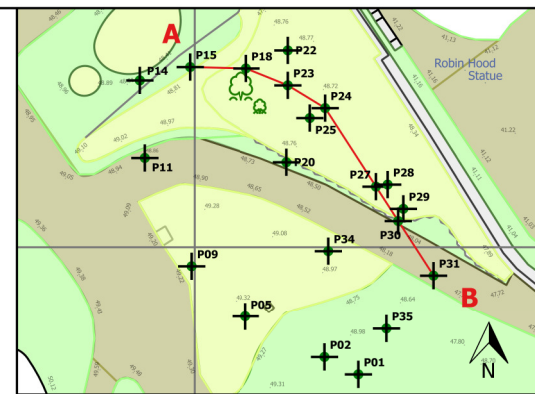
Key

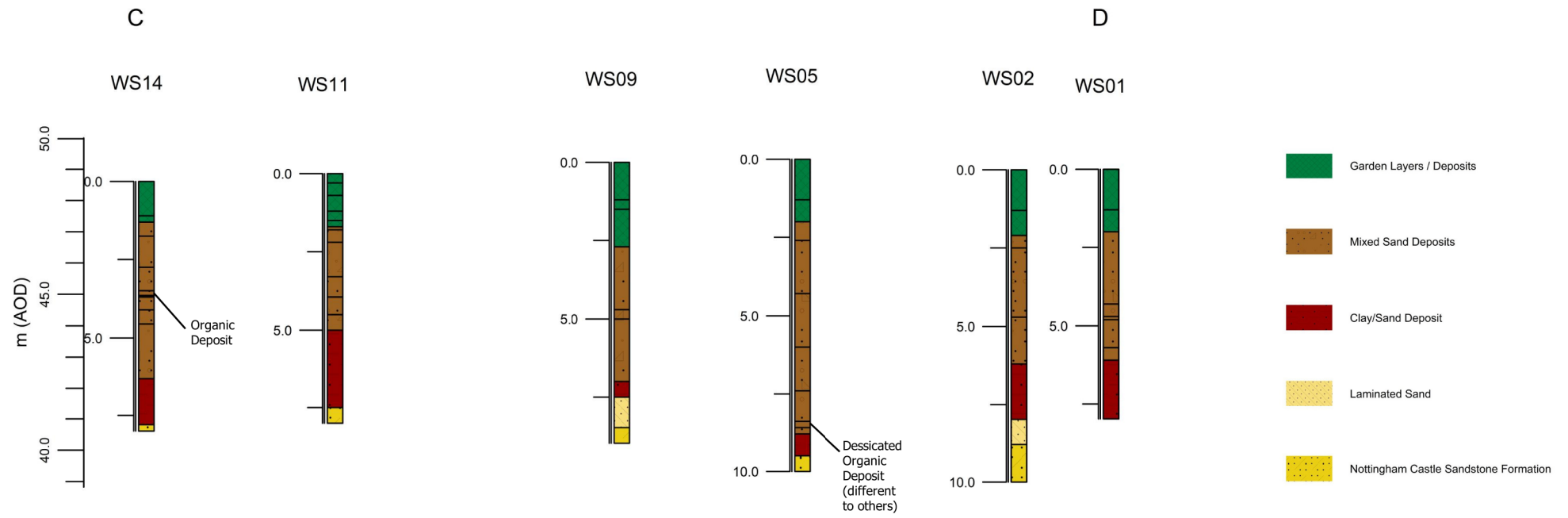
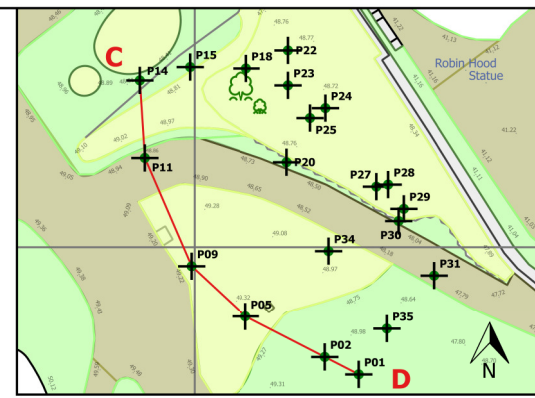
- ✚ Window Sample
- Height of Unit A (m AOD)
 - 37.99
 - 38.75
 - 39.51
 - 40.27
 - 41.03
- 48.50 Present Ground Surface Spot Heights (m AOD)

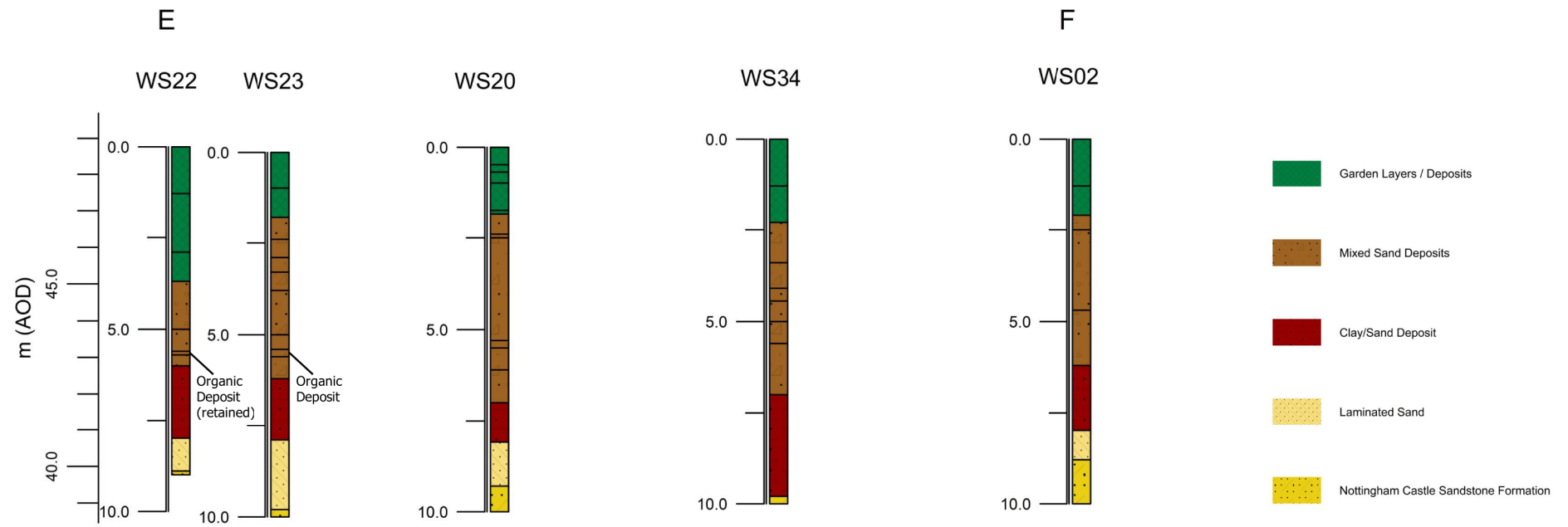
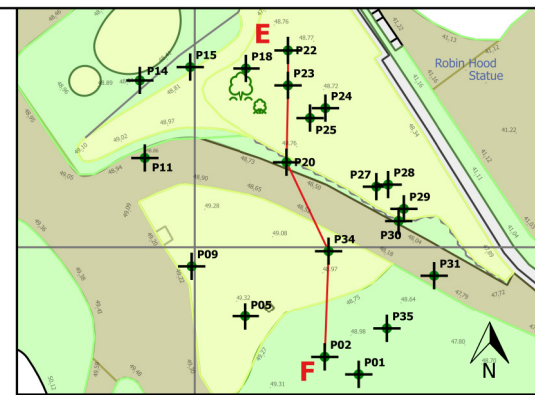


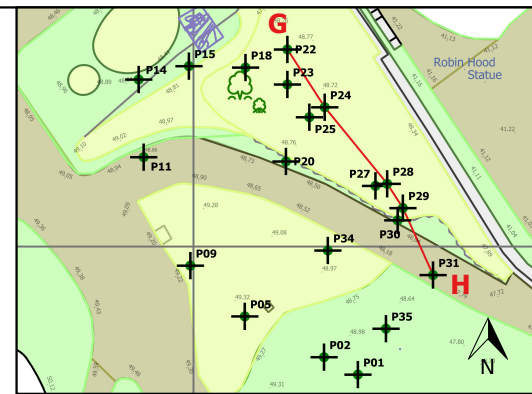
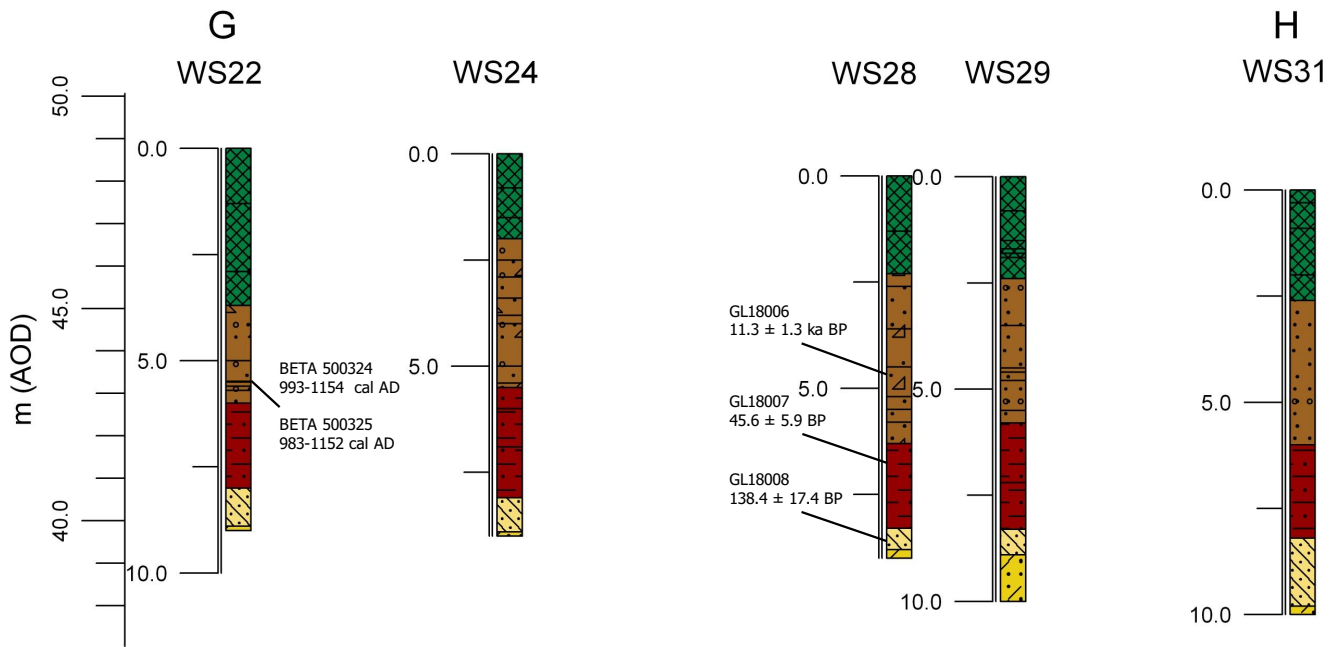
Key






- ✚ Window Sample
- Height of Unit C (m AOD)
 - 40.34
 - 41.22
 - 42.1
 - 42.98
 - 43.86
- 48.50 Present Ground Surface Spot Heights (m AOD)









-  Garden Layers / Deposits
-  Mixed Sand Deposits
-  Clay/Sand Deposit
-  Laminated Sand
-  Nottingham Castle Sandstone Formation

7. Appendix



Beta Analytic
RADIOCARBON DATING

Beta Analytic Inc
4985 SW 74 Court
Miami, Florida 33155
Tel: 305-667-5167
Fax: 305-663-0964
beta@radiocarbon.com

Mr. Darden Hood
President

Mr. Ronald Hatfield
Mr. Christopher Patrick
Deputy Directors

ISO/IEC 17025:2005 Accredited Test Results. Testing results recognized by all Signatories to the ILAC Mutual Recognition Arrangement

August 14, 2018

Dr. Kristina Krawiec
Trent and Peak Archaeology
Unit 1, Holly Lane, Chilwell
Nottingham, NG9 4AB
United Kingdom

RE: Radiocarbon Dating Results

Dear Dr. Krawiec,

Enclosed are the radiocarbon dating results for two samples recently sent to us. As usual, the method of analysis is listed on the report with the results and calibration data is provided where applicable. The Conventional Radiocarbon Ages have all been corrected for total fractionation effects and where applicable, calibration was performed using 2013 calibration databases (cited on the graph pages).

The web directory containing the table of results and PDF download also contains pictures, a cvs spreadsheet download option and a quality assurance report containing expected vs. measured values for 3-5 working standards analyzed simultaneously with your samples.

Reported results are accredited to ISO/IEC 17025:2005 Testing Accreditation PJLA #50423 standards and all chemistry was performed here in our laboratory and counted in our own accelerators here. Since Beta is not a teaching laboratory, only graduates trained to strict protocols of the ISO/IEC 17025:2005 Testing Accreditation PJLA #50423 program participated in the analyses.

As always Conventional Radiocarbon Ages and sigmas are rounded to the nearest 10 years per the conventions of the 1977 International Radiocarbon Conference. When counting statistics produce sigmas lower than +/- 30 years, a conservative +/- 30 BP is cited for the result. The reported $\delta^{13}C$ values were measured separately in an IRMS (isotope ratio mass spectrometer). They are NOT the AMS $\delta^{13}C$ which would include fractionation effects from natural, chemistry and AMS induced sources.

When interpreting the results, please consider any communications you may have had with us regarding the samples.

Our invoice will be emailed separately. Please forward it to the appropriate officer or send a credit card authorization. Thank you. As always, if you have any questions or would like to discuss the results, don't hesitate to contact us.

Sincerely,

A handwritten signature in black ink that reads "Darden Hood". Below the signature, the text "DARDEN HOOD" is printed in a small, sans-serif font.



Beta Analytic
RADIOCARBON DATING

Beta Analytic Inc
4985 SW 74 Court
Miami, Florida 33155
Tel: 305-667-5167
Fax: 305-663-0964
beta@radiocarbon.com

Mr. Darden Hood
President

Mr. Ronald Hatfield
Mr. Christopher Patrick
Deputy Directors

ISO/IEC 17025:2005-Accredited Testing Laboratory

REPORT OF RADIOCARBON DATING ANALYSES

Kristina Krawiec

Report Date: August 14, 2018

Trent and Peak Archaeology

Material Received: July 26, 2018

Laboratory Number	Sample Code Number	Conventional Radiocarbon Age (BP) or Percent Modern Carbon (pMC) & Stable Isotopes	
		Calendar Calibrated Results: 95.4 % Probability High Probability Density Range Method (HPD)	
Beta - 500324	TPA_023 Humic	980 +/- 30 BP	IRMS δ13C: -27.6 ‰

(49.4%) 1070 - 1154 cal AD (880 - 796 cal BP)
(46.0%) 993 - 1058 cal AD (957 - 892 cal BP)

Submitter Material: Organic Sediment/Gyttja
Pretreatment: (alkali soluble organics) acid/alkali/acid

Analyzed Material: Alkali soluble organics
Analysis Service: AMS-Standard delivery

Percent Modern Carbon: 88.52 +/- 0.33 pMC

Fraction Modern Carbon: 0.8852 +/- 0.0033

D14C: -114.85 +/- 3.31 ‰

Δ14C: -122.10 +/- 3.31 ‰(1950:2,018.00)

Measured Radiocarbon Age: (without δ13C correction): 1020 +/- 30 BP

Calibration: BetaCal3.21: HPD method: INTCAL13

Results are ISO/IEC-17025:2005 accredited. No sub-contracting or student labor was used in the analyses. All work was done at Beta in 4 in-house NEC accelerator mass spectrometers and 4 Thermo RMSs. The "Conventional Radiocarbon Age" was calculated using the Libby half-life (5568 years), is corrected for total isotopic fraction and was used for calendar calibration where applicable. The Age is rounded to the nearest 10 years and is reported as radiocarbon years before present (BP), "present" = AD 1950. Results greater than the modern reference are reported as percent modern carbon (pMC). The modern reference standard was 95% the 14C signature of NIST SRM-4900C (oxalic acid). Quoted errors are 1 sigma counting statistics. Calculated sigmas less than 30 BP on the Conventional Radiocarbon Age are conservatively rounded up to 30. δ13C values are on the material itself (not the AMS δ13C). δ13C and δ15N values are relative to VPDB-1. References for calendar calibrations are cited at the bottom of calibration graph pages.



Beta Analytic
RADIOCARBON DATING

Beta Analytic Inc
4985 SW 74 Court
Miami, Florida 33155
Tel: 305-667-5167
Fax: 305-663-0964
beta@radiocarbon.com

Mr. Darden Hood
President

Mr. Ronald Hatfield
Mr. Christopher Patrick
Deputy Directors

ISO/IEC 17025:2005-Accredited Testing Laboratory

REPORT OF RADIOCARBON DATING ANALYSES

Kristina Krawiec

Report Date: August 14, 2018

Trent and Peak Archaeology

Material Received: July 26, 2018

Laboratory Number	Sample Code Number	Conventional Radiocarbon Age (BP) or Percent Modern Carbon (pMC) & Stable Isotopes	
		Calendar Calibrated Results: 95.4 % Probability High Probability Density Range Method (HPD)	
Beta - 500325	TPA_024 Humin	1000 +/- 30 BP	IRMS δ13C: -26.1 o/oo
	(71.0%) 983 - 1051 cal AD	(967 - 899 cal BP)	
	(19.2%) 1082 - 1128 cal AD	(868 - 822 cal BP)	
	(5.2%) 1135 - 1152 cal AD	(815 - 798 cal BP)	
	Submitter Material: Organic Sediment/Gyttja		
	Pretreatment: (alkali insoluble organics) acid/alkali/acid		
	Analyzed Material: Alkali insoluble organics		
	Analysis Service: AMS-Standard delivery		
	Percent Modern Carbon: 88.29 +/- 0.33 pMC		
	Fraction Modern Carbon: 0.8829 +/- 0.0033		
	D14C: -117.05 +/- 3.30 o/oo		
	Δ14C: -124.28 +/- 3.30 o/oo(1950:2,018.00)		
	Measured Radiocarbon Age: (without δ13C correction): 1020 +/- 30 BP		
	Calibration: BetaCal3.21: HPD method: INTCAL13		

Results are ISO/IEC-17025:2005 accredited. No sub-contracting or student labor was used in the analyses. All work was done at Beta in 4 in-house NEC accelerator mass spectrometers and 4 Thermo IRMSs. The "Conventional Radiocarbon Age" was calculated using the Libby half-life (5568 years), is corrected for total isotopic fraction and was used for calendar calibration where applicable. The Age is rounded to the nearest 10 years and is reported as radiocarbon years before present (BP), "present" = AD 1950. Results greater than the modern reference are reported as percent modern carbon (pMC). The modern reference standard was 95% the ¹⁴C signature of NIST SRM-4900C (oxalic acid). Quoted errors are 1 sigma counting statistics. Calculated sigmas less than 30 BP on the Conventional Radiocarbon Age are conservatively rounded up to 30. δ13C values are on the material itself (not the AMS δ13C). δ13C and δ15N values are relative to VPDB-1. References for calendar calibrations are cited at the bottom of calibration graph pages.

BetaCal 3.21

Calibration of Radiocarbon Age to Calendar Years

(High Probability Density Range Method (HPD): INTCAL13)

(Variables: $\delta^{13}C = -27.6$ o/oo)

Laboratory number Beta-500324

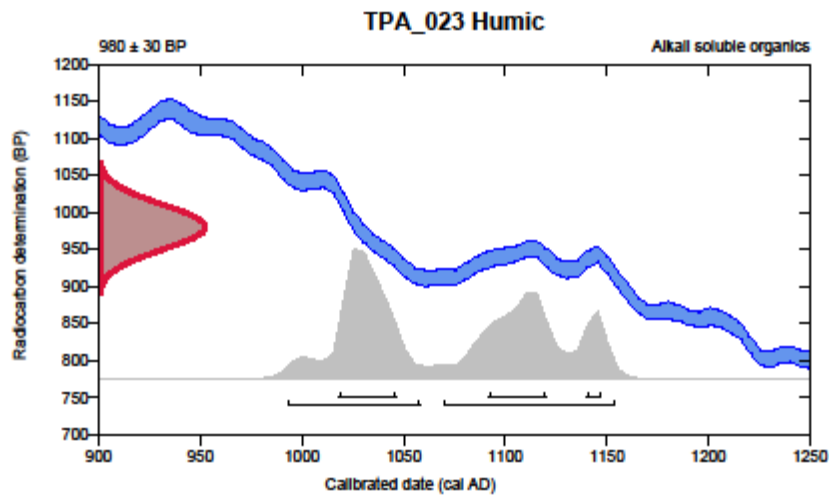
Conventional radiocarbon age 980 ± 30 BP

95.4% probability

(49.4%)	1070 - 1154 cal AD	(880 - 796 cal BP)
(46%)	993 - 1058 cal AD	(957 - 892 cal BP)

68.2% probability

(36.6%)	1018 - 1046 cal AD	(932 - 904 cal BP)
(26%)	1092 - 1120 cal AD	(858 - 830 cal BP)
(5.6%)	1140 - 1147 cal AD	(810 - 803 cal BP)



Database used

INTCAL13

References

References to Probability Method

Bronk Ramsey, C. (2009). Bayesian analysis of radiocarbon dates. *Radiocarbon*, 51(1), 337-360.

References to Database INTCAL13

Reimer, et.al., 2013, *Radiocarbon*55(4).

Beta Analytic Radiocarbon Dating Laboratory

4985 S.W. 74th Court, Miami, Florida 33155 • Tel: (305)867-5167 • Fax: (305)863-0984 • Email: beta@radiocarbon.com

BetaCal 3.21

Calibration of Radiocarbon Age to Calendar Years

(High Probability Density Range Method (HPD): INTCAL13)

(Variables: $\delta^{13}\text{C} = -26.1$ o/oo)

Laboratory number Beta-500325

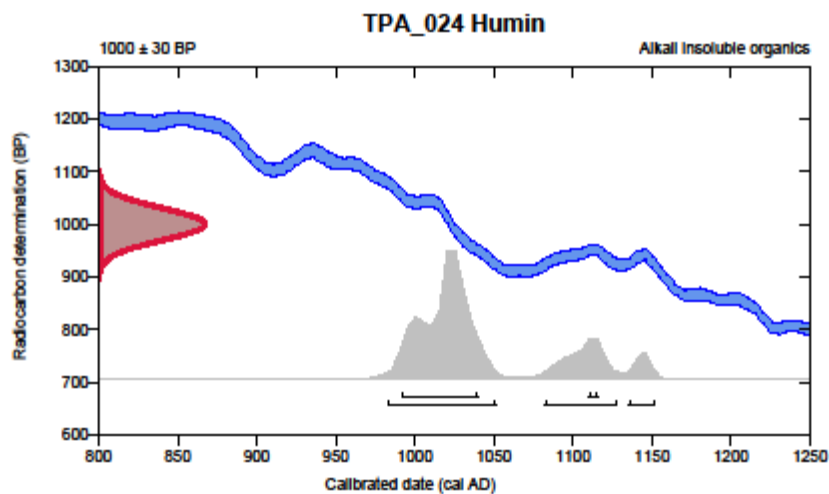
Conventional radiocarbon age 1000 ± 30 BP

95.4% probability

(71%)	983 - 1051 cal AD	(967 - 899 cal BP)
(19.2%)	1082 - 1128 cal AD	(868 - 822 cal BP)
(5.2%)	1135 - 1152 cal AD	(815 - 798 cal BP)

68.2% probability

(63.9%)	992 - 1040 cal AD	(958 - 910 cal BP)
(4.3%)	1110 - 1116 cal AD	(840 - 834 cal BP)



Database used

INTCAL13

References

References to Probability Method

Bronk Ramsey, C. (2009). Bayesian analysis of radiocarbon dates. *Radiocarbon*, 51(1), 337-360.

References to Database INTCAL13

Reimer, et.al., 2013, *Radiocarbon*55(4).

Beta Analytic Radiocarbon Dating Laboratory

4985 S.W. 74th Court, Miami, Florida 33155 • Tel: (305)867-5167 • Fax: (305)863-0984 • Email: beta@radiocarbon.com



Beta Analytic
RADIOCARBON DATING

Beta Analytic Inc
4985 SW 74 Court
Miami, Florida 33155
Tel: 305-667-5167
Fax: 305-663-0964
beta@radiocarbon.com

Mr. Darden Hood
President

Mr. Ronald Hatfield
Mr. Christopher Patrick
Deputy Directors

ISO/IEC 2005:17025-Accredited Testing Laboratory

Quality Assurance Report

This report provides the results of reference materials used to validate radiocarbon analyses prior to reporting. Known-value reference materials were analyzed quasi-simultaneously with the unknowns. Results are reported as expected values vs measured values. Reported values are calculated relative to NIST SRM-4990B and corrected for isotopic fractionation. Results are reported using the direct analytical measure percent modern carbon (pMC) with one relative standard deviation. Agreement between expected and measured values is taken as being within 2 sigma agreement (error x 2) to account for total laboratory error.

Report Date: August 14, 2018
Submitter: Dr. Kristina Krawiec

QA MEASUREMENTS

Reference 1

Expected Value: 129.41 +/- 0.06 pMC
Measured Value: 129.47 +/- 0.35 pMC
Agreement: Accepted

Reference 2

Expected Value: 98.89 +/- 0.50 pMC
Measured Value: 98.81 +/- 0.28 pMC
Agreement: Accepted

Reference 3

Expected Value: 0.49 +/- 0.10 pMC
Measured Value: 0.50 +/- 0.03 pMC
Agreement: Accepted

COMMENT: All measurements passed acceptance tests.

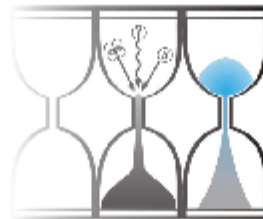
Validation:

Date: August 14, 2018



University of Gloucestershire

Luminescence dating laboratory



Optical dating of sediments: Nottingham Castle borehole

to

K. Krawiec

Trent & Peak Archaeology

**Analysis & Reporting, Dr P.S. Toms
Sample Preparation & Measurement, Mr J.C. Wood
30 October 2018**

Contents

Section		Page
	Table 1 D_e , D_o and Age data of submitted samples	3
	Table 2 Analytical validity of sample suite ages	4
1.0	Mechanisms and Principles	5
2.0	Sample Preparation	5
3.0	Acquisition and accuracy of D_e value	6
	3.1 Laboratory Factors	6
	3.1.1 Feldspar Contamination	6
	3.1.2 Preheating	6
	3.1.3 Irradiation	7
	3.1.4 Internal Consistency	7
	3.2 Environmental Factors	7
	3.2.1 Incomplete Zeroing	7
	3.2.2 Turbation	8
4.0	Acquisition and accuracy of D_o value	8
5.0	Estimation of age	9
6.0	Analytical Uncertainty	9
	Sample diagnostics, luminescence and age data	12
	References	15

Scope of Report

This is a standard report of the Luminescence dating laboratory, University of Gloucestershire. In large part, the document summarises the processes, diagnostics and data drawn upon to deliver Table 1. A conclusion on the analytical validity of each sample's optical age estimate is expressed in Table 2; where there are caveats, the reader is directed to the relevant section of the report that explains the issue further in general terms.

Copyright Notice

Permission must be sought from Dr P.S. Toms of the University of Gloucestershire Luminescence dating laboratory in using the content of this report, in part or whole, for the purpose of publication.

Field Code	Lab Code	Overburden (m)	Grain size (µm)	Moisture content (%)	Gr _e -spectrometry (w/alt)			g D _e (Gy.kt ⁻¹)	γ D _e (Gy.kt ⁻¹)	Cosmic D _e (Gy.kt ⁻¹)	Preheat (°C for 10s)	Low Dose Repeat Ratio	Dose rate applied Low Regenerative dose D _e	High Dose Repeat Ratio	Dose rate applied High Regenerative dose D _e	Final OSL Ratio
					K (%)	Tn (ppm)	U (ppm)									
NCA14 - WS28: 4-5 m	GL18006	4.94	180-250	4 ± 1	1.87 ± 0.12	3.83 ± 0.37	1.01 ± 0.11	1.49 ± 0.15	0.71 ± 0.11	0.10 ± 0.01	240	1.00 ± 0.07	1.00 ± 0.05	1.02 ± 0.05	1.05 ± 0.06	0.94 ± 0.06
NCA14 - WS28: 6-7 m	GL18007	8.86	180-250	7 ± 2	1.78 ± 0.11	7.96 ± 0.52	1.80 ± 0.14	1.51 ± 0.14	0.93 ± 0.11	0.08 ± 0.01	240	1.08 ± 0.10	1.08 ± 0.08	1.02 ± 0.08	1.07 ± 0.08	0.91 ± 0.08
NCA14 - WS28: 8-9 m	GL18008	8.81	180-250	5 ± 1	2.41 ± 0.14	5.18 ± 0.42	0.94 ± 0.12	1.84 ± 0.18	0.88 ± 0.14	0.08 ± 0.01	260	1.03 ± 0.08	1.04 ± 0.08	0.96 ± 0.04	0.87 ± 0.08	0.85 ± 0.08

Field Code	Lab Code	Total D _e (Gy.kt ⁻¹)	D _e (Gy)	Age (ka)
NCA14 - WS28: 4-5 m	GL18006	2.29 ± 0.15	25.9 ± 2.5	11.3 ± 1.3 (1.2)
NCA14 - WS28: 6-7 m	GL18007	2.51 ± 0.16	114.6 ± 13.0	45.6 ± 5.9 (5.5)
NCA14 - WS28: 8-9 m	GL18008	2.79 ± 0.19	385.8 ± 40.8	138.4 ± 17.4 (15.6)

Table 1 D_e, D_e and Age data of submitted samples located at c. 53°N, 1°W, 40m. Age estimates expressed relative to year of sampling. Uncertainties in age are quoted at 1σ confidence, are based on analytical errors and reflect combined systematic and experimental variability and (in parenthesis) experimental variability alone (see 6.0). **Blue** indicates samples with accepted age estimates, **red**, age estimates with caveats (see Table 2).

Generic considerations	Field Code	Lab Code	Sample specific considerations
Absence of <i>in situ</i> γ spectrometry data (see section 4.0)	NCA14 - WS28: 4-5 m	GL18006	None
	NCA14 - WS28: 6-7 m	GL18007	None
	NCA14 - WS28: 8-9 m	GL18008	Failed Dose Recovery Test (see section 3.1.2 and Fig. 1) Potentially significant feldspar contamination (see section 3.1.1, Table 1 and Fig. 1) Accept as minimum age estimate

Table 2 Analytical validity of sample suite age estimates and caveats for consideration

1.0 Mechanisms and principles

Upon exposure to ionising radiation, electrons within the crystal lattice of insulating minerals are displaced from their atomic orbits. Whilst this dislocation is momentary for most electrons, a portion of charge is redistributed to meta-stable sites (traps) within the crystal lattice. In the absence of significant optical and thermal stimuli, this charge can be stored for extensive periods. The quantity of charge relocation and storage relates to the magnitude and period of irradiation. When the lattice is optically or thermally stimulated, charge is evicted from traps and may return to a vacant orbit position (hole). Upon recombination with a hole, an electron's energy can be dissipated in the form of light generating crystal luminescence providing a measure of dose absorption.

Herein, quartz is segregated for dating. The utility of this minerogenic dosimeter lies in the stability of its datable signal over the mid to late Quaternary period, predicted through isothermal decay studies (e.g. Smith *et al.*, 1990; retention lifetime 630 Ma at 20°C) and evidenced by optical age estimates concordant with independent chronological controls (e.g. Murray and Olley, 2002). This stability is in contrast to the anomalous fading of comparable signals commonly observed for other ubiquitous sedimentary minerals such as feldspar and zircon (Wintle, 1973; Templer, 1985; Spooner, 1993)

Optical age estimates of sedimentation (Huntley *et al.*, 1985) are premised upon reduction of the minerogenic time dependent signal (Optically Stimulated Luminescence, OSL) to zero through exposure to sunlight and, once buried, signal reformulation by absorption of litho- and cosmogenic radiation. The signal accumulated post burial acts as a dosimeter recording total dose absorption, converting to a chronometer by estimating the rate of dose absorption quantified through the assay of radioactivity in the surrounding lithology and streaming from the cosmos.

$$\text{Age} = \frac{\text{Mean Equivalent Dose (D}_e\text{, Gy)}}{\text{Mean Dose Rate (D}_i\text{, Gy.ka}^{-1}\text{)}}$$

Aitken (1998) and Bøtter-Jensen *et al.* (2003) offer a detailed review of optical dating.

2.0 Sample Preparation

Three borehole sediment samples were collected within opaque tubing and submitted for Optical dating. To preclude optical erosion of the datable signal prior to measurement, all samples were opened and prepared under controlled laboratory illumination provided by Encapsulite RB-10 (red) filters. To isolate that material potentially exposed to daylight during sampling, sediment located within 10 mm of each core face was removed.

The remaining sample was dried and then sieved. The fine sand fraction was segregated and subjected to acid and alkaline digestion (10% HCl, 15% H₂O₂) to attain removal of carbonate and organic components respectively. A further acid digestion in HF (40%, 60 mins) was used to etch the outer 10-15 µm layer affected by α radiation and degrade each samples' feldspar content. During HF treatment, continuous magnetic stirring was used to effect isotropic etching of grains. 10% HCl was then added to remove acid soluble fluorides. Each sample was dried, resieved and quartz isolated from the remaining heavy mineral fraction using a sodium polytungstate density separation at 2.68g.cm⁻³. Twelve 8 mm multi-grain aliquots (c. 3-6 mg) of quartz from each sample were then mounted on aluminium discs for determination of D_e values.

All drying was conducted at 40°C to prevent thermal erosion of the signal. All acids and alkalis were Analar grade. All dilutions (removing toxic-corrosive and non-minerogenic luminescence-bearing substances) were conducted with distilled water to prevent signal contamination by extraneous particles.

3.0 Acquisition and accuracy of D_e value

All minerals naturally exhibit marked inter-sample variability in luminescence per unit dose (sensitivity). Therefore, the estimation of D_e acquired since burial requires calibration of the natural signal using known amounts of laboratory dose. D_e values were quantified using a single-aliquot regenerative-dose (SAR) protocol (Murray and Wintle 2000; 2003) facilitated by a Rise TL-DA-15 irradiation-stimulation-detection system (Markey *et al.*, 1997; Bøtter-Jensen *et al.*, 1999). Within this apparatus, optical signal stimulation is provided by an assembly of blue diodes (5 packs of 6 Nichia NSPB500S), filtered to 470 ± 80 nm conveying $15 \text{ mW}\cdot\text{cm}^{-2}$ using a 3 mm Schott GG420 positioned in front of each diode pack. Infrared (IR) stimulation, provided by 6 IR diodes (Telefunken TSHA 6203) stimulating at 875 ± 80 nm delivering $\sim 5 \text{ mW}\cdot\text{cm}^{-2}$, was used to indicate the presence of contaminant feldspars (Hütt *et al.*, 1988). Stimulated photon emissions from quartz aliquots are in the ultraviolet (UV) range and were filtered from stimulating photons by 7.5 mm HOYA U-340 glass and detected by an EMI 9235QA photomultiplier fitted with a blue-green sensitive bialkali photocathode. Aliquot irradiation was conducted using a $1.48 \text{ GBq } ^{60}\text{Sr}/^{60}\text{Y}$ β source calibrated for multi-grain aliquots of 180-250 μm quartz against the 'Hotspot 800' ^{60}Co γ source located at the National Physical Laboratory (NPL), UK.

SAR by definition evaluates D_e through measuring the natural signal (Fig. 1) of a single aliquot and then regenerating that aliquot's signal by using known laboratory doses to enable calibration. For each aliquot, five different regenerative-doses were administered so as to image dose response. D_e values for each aliquot were then interpolated, and associated counting and fitting errors calculated, by way of exponential plus linear regression (Fig. 1). Weighted (geometric) mean D_e values were calculated from 12 aliquots using the central age model outlined by Galbraith *et al.* (1999) and are quoted at 1σ confidence (Table 1). The accuracy with which D_e equates to total absorbed dose and that dose absorbed since burial was assessed. The former can be considered a function of laboratory factors, the latter, one of environmental issues. Diagnostics were deployed to estimate the influence of these factors and criteria instituted to optimise the accuracy of D_e values.

3.1 Laboratory Factors

3.1.1 Feldspar contamination

The propensity of feldspar signals to fade and underestimate age, coupled with their higher sensitivity relative to quartz makes it imperative to quantify feldspar contamination. At room temperature, feldspars generate a signal (IRSL; Fig. 1) upon exposure to IR whereas quartz does not. The signal from feldspars contributing to OSL can be depleted by prior exposure to IR. For all aliquots the contribution of any remaining feldspars was estimated from the OSL IR depletion ratio (Duller, 2003). The influence of IR depletion on the OSL signal can be illustrated by comparing the regenerated post-IR OSL D_e with the applied regenerative-dose. If the addition to OSL by feldspars is insignificant, then the repeat dose ratio of OSL to post-IR OSL should be statistically consistent with unity (Table 1). If any aliquots do not fulfil this criterion, then the sample age estimate should be accepted tentatively. The source of feldspar contamination is rarely rooted in sample preparation; it predominantly results from the occurrence of feldspars as inclusions within quartz.

3.1.2 Preheating

Preheating aliquots between irradiation and optical stimulation is necessary to ensure comparability between natural and laboratory-induced signals. However, the multiple irradiation and preheating steps that are required to define single-aliquot regenerative-dose response leads to signal sensitisation, rendering calibration of the natural signal inaccurate. The SAR protocol (Murray and Wintle, 2000; 2003) enables this sensitisation to be monitored and corrected using a test dose, here set at 5 Gy preheated to 220°C for 10s, to track signal sensitivity between irradiation-preheat steps. However, the accuracy of sensitisation correction for both natural and laboratory signals can be preheat dependent.

The Dose Recovery test was used to assess the optimal preheat temperature for accurate correction and calibration of the time dependent signal. Dose Recovery (Fig. 2) attempts to quantify the combined effects of thermal transfer and

sensitisation on the natural signal, using a precise lab dose to simulate natural dose. The ratio between the applied dose and recovered D_e value should be statistically concordant with unity. For this diagnostic, 6 aliquots were each assigned a 10 s preheat between 180°C and 280°C.

That preheat treatment fulfilling the criterion of accuracy within the Dose Recovery test was selected to generate the final D_e value from a further 12 aliquots. Further thermal treatments, prescribed by Murray and Wintle (2000; 2003), were applied to optimise accuracy and precision. Optical stimulation occurred at 125°C in order to minimise effects associated with photo-transferred thermoluminescence and maximise signal to noise ratios. Inter-cycle optical stimulation was conducted at 280°C to minimise recuperation.

3.1.3 Irradiation

For all samples having D_e values in excess of 100 Gy, matters of signal saturation and laboratory irradiation effects are of concern. With regards the former, the rate of signal accumulation generally adheres to a saturating exponential form and it is this that limits the precision and accuracy of D_e values for samples having absorbed large doses. For such samples, the functional range of D_e interpolation by SAR has been verified up to 600 Gy by Pawley *et al.* (2010). Age estimates based on D_e values exceeding this value should be accepted tentatively.

3.1.4 Internal consistency

Abanico plots (Dietze *et al.*, 2016) are used to illustrate inter-aliquot D_e variability (Fig. 3). D_e values are standardised relative to the central D_e value for natural signals and are described as overdispersed when >5% lie beyond $\pm 2\sigma$ of the standardising value; resulting from a heterogeneous absorption of burial dose and/or response to the SAR protocol. For multi-grain aliquots, overdispersion of natural signals does not necessarily imply inaccuracy. However where overdispersion is observed for regenerated signals, the efficacy of sensitivity correction may be problematic. Murray and Wintle (2000; 2003) suggest repeat dose ratios (Table 1) offer a measure of SAR protocol success, whereby ratios ranging across 0.9-1.1 are acceptable. However, this variation of repeat dose ratios in the high-dose region can have a significant impact on D_e interpolation. The influence of this effect can be outlined by quantifying the ratio of interpolated to applied regenerative-dose ratio (Table 1). In this study, where both the repeat dose ratios and interpolated to applied regenerative-dose ratios range across 0.9-1.1, sensitivity-correction is considered effective.

3.2 Environmental factors

3.2.1 Incomplete zeroing

Post-burial OSL signals residual of pre-burial dose absorption can result where pre-burial sunlight exposure is limited in spectrum, intensity and/or period, leading to age overestimation. This effect is particularly acute for material eroded and redeposited sub-aqueously (Olley *et al.*, 1998, 1999; Wallinga, 2002) and exposed to a burial dose of <20 Gy (e.g. Olley *et al.*, 2004), has some influence in sub-aerial contexts but is rarely of consequence where aerial transport has occurred. Within single-aliquot regenerative-dose optical dating there are two diagnostics of partial resetting (or bleaching): signal analysis (Agersnap-Larsen *et al.*, 2000; Bailey *et al.*, 2003) and inter-aliquot D_e distribution studies (Murray *et al.*, 1995).

Within this study, signal analysis was used to quantify the change in D_e value with respect to optical stimulation time for multi-grain aliquots. This exploits the existence of traps within minerogenic dosimeters that bleach with different efficiency for a given wavelength of light to verify partial bleaching. $D_e(t)$ plots (Fig. 4; Bailey *et al.*, 2003) are constructed from separate integrals of signal decay as laboratory optical stimulation progresses. A statistically significant increase in natural $D_e(t)$ is indicative of partial bleaching assuming three conditions are fulfilled. Firstly, that a statistically significant increase in $D_e(t)$ is observed when partial bleaching is simulated within the laboratory. Secondly, that there is no significant rise in $D_e(t)$ when full bleaching is simulated. Finally, there should be no significant augmentation in $D_e(t)$ when zero dose is simulated. Where partial bleaching is detected, the age derived from the sample should be considered a maximum estimate only. However, the utility of signal analysis is strongly dependent upon a samples pre-burial

experience of sunlight's spectrum and its residual to post-burial signal ratio. Given in the majority of cases, the spectral exposure history of a deposit is uncertain, the absence of an increase in natural $D_e(t)$ does not necessarily testify to the absence of partial bleaching.

Where requested and feasible, the insensitivities of multi-grain single-aliquot signal analysis may be circumvented by inter-aliquot D_e distribution studies. This analysis uses aliquots of single sand grains to quantify inter-grain D_e distribution. At present, it is contended that asymmetric inter-grain D_e distributions are symptomatic of partial bleaching and/or pedoturbation (Murray *et al.*, 1995; Olley *et al.*, 1999; Olley *et al.*, 2004; Bateman *et al.*, 2003). For partial bleaching at least, it is further contended that the D_e acquired during burial is located in the minimum region of such ranges. The mean and breadth of this minimum region is the subject of current debate, as it is additionally influenced by heterogeneity in microdosimetry, variable inter-grain response to SAR and residual to post-burial signal ratios.

3.2.2 Turbation

As noted in section 3.1.1, the accuracy of sedimentation ages can further be controlled by post-burial trans-strata grain movements forced by pedo- or cryoturbation. Berger (2003) contends pedogenesis prompts a reduction in the apparent sedimentation age of parent material through bioturbation and illuviation of younger material from above and/or by biological recycling and resetting of the datable signal of surface material. Berger (2003) proposes that the chronological products of this remobilisation are A-horizon age estimates reflecting the cessation of pedogenic activity, Bc/C-horizon ages delimiting the maximum age for the initiation of pedogenesis with estimates obtained from Bt-horizons providing an intermediate age 'close to the age of cessation of soil development'. Singhvi *et al.* (2001), in contrast, suggest that B and C-horizons closely approximate the age of the parent material, the A-horizon, that of the 'soil forming episode'. Recent analyses of inter-aliquot D_e distributions have reinforced this complexity of interpreting burial age from pedoturbated deposits (Lombard *et al.*, 2011; Gliganic *et al.*, 2015; Jacobs *et al.*, 2008; Bateman *et al.*, 2007; Gliganic *et al.*, 2016). At present there is no definitive post-sampling mechanism for the direct detection of and correction for post-burial sediment remobilisation. However, intervals of palaeosol evolution can be delimited by a maximum age derived from parent material and a minimum age obtained from a unit overlying the palaeosol. Inaccuracy forced by cryoturbation may be bidirectional, heaving older material upwards or drawing younger material downwards into the level to be dated. Cryogenic deformation of matrix-supported material is, typically, visible; sampling of such cryogenically-disturbed sediments can be avoided.

4.0 Acquisition and accuracy of D_r value

Lithogenic D_r values were defined through measurement of U, Th and K radionuclide concentration and conversion of these quantities into β and γ D_r values (Table 1). β contributions were estimated from sub-samples by laboratory-based γ spectrometry using an Ortec GEM-S high purity Ge coaxial detector system, calibrated using certified reference materials supplied by CANMET. γ dose rates can be estimated from *in situ* NaI gamma spectrometry or, where direct measurements are unavailable as in the present case, from laboratory-based Ge γ spectrometry. *In situ* measurements reduce uncertainty relating to potential heterogeneity in the γ dose field surrounding each sample. The level of U disequilibrium was estimated by laboratory-based Ge γ spectrometry. Estimates of radionuclide concentration were converted into D_r values (Adamiec and Aitken, 1998), accounting for D_r modulation forced by grain size (Mejdahl, 1979) and present moisture content (Zimmerman, 1971). Cosmogenic D_r values were calculated on the basis of sample depth, geographical position and matrix density (Prescott and Hutton, 1994).

The spatiotemporal validity of D_r values can be considered a function of five variables. Firstly, age estimates devoid of *in situ* γ spectrometry data should be accepted tentatively if the sampled unit is heterogeneous in texture or if the sample is located within 300 mm of strata consisting of differing texture and/or mineralogy. However, where samples are obtained

throughout a vertical profile, consistent values of γD_r based solely on laboratory measurements may evidence the homogeneity of the γ field and hence accuracy of γD_r values. Secondly, disequilibrium can force temporal instability in U and Th emissions. The impact of this infrequent phenomenon (Olley *et al.*, 1996) upon age estimates is usually insignificant given their associated margins of error. However, for samples where this effect is pronounced (>50% disequilibrium between ^{238}U and ^{226}Ra ; Fig. 5), the resulting age estimates should be accepted tentatively. Thirdly, pedogenically-induced variations in matrix composition of B and C-horizons, such as radionuclide and/or mineral remobilisation, may alter the rate of energy emission and/or absorption. If D_r is invariant through a dated profile and samples encompass primary parent material, then element mobility is likely limited in effect. Fourthly, spatiotemporal detractions from present moisture content are difficult to assess directly, requiring knowledge of the magnitude and timing of differing contents. However, the maximum influence of moisture content variations can be delimited by recalculating D_r for minimum (zero) and maximum (saturation) content. Finally, temporal alteration in the thickness of overburden alters cosmic D_r values. Cosmic D_r often forms a negligible portion of total D_r . It is possible to quantify the maximum influence of overburden flux by recalculating D_r for minimum (zero) and maximum (surface sample) cosmic D_r .

5.0 Estimation of Age

Ages reported in Table 1 provide an estimate of sediment burial period based on mean D_e and D_r values and their associated analytical uncertainties. Uncertainty in age estimates is reported as a product of systematic and experimental errors, with the magnitude of experimental errors alone shown in parenthesis (Table 1). Cumulative frequency plots indicate the inter-aliquot variability in age (Fig. 6). The maximum influence of temporal variations in D_r forced by minima-maxima in moisture content and overburden thickness is also illustrated in Fig. 6. Where uncertainty in these parameters exists this age range may prove instructive, however the combined extremes represented should not be construed as preferred age estimates. The analytical validity of each sample is presented in Table 2.

6.0 Analytical uncertainty

All errors are based upon analytical uncertainty and quoted at 1σ confidence. Error calculations account for the propagation of systematic and/or experimental (random) errors associated with D_e and D_r values.

For D_e values, systematic errors are confined to laboratory β source calibration. Uncertainty in this respect is that combined from the delivery of the calibrating γ dose (1.2%; NPL, pers. comm.), the conversion of this dose for SiO_2 using the respective mass energy-absorption coefficient (2%; Hubbell, 1982) and experimental error, totalling 3.5% 2.4%. Mass attenuation and bremsstrahlung losses during γ dose delivery are considered negligible. Experimental errors relate to D_e interpolation using sensitisation corrected dose responses. Natural and regenerated sensitisation corrected dose points (S_i) were quantified by,

$$S_i = (D_i - x.L_i) / (d_i - x.L_i) \quad \text{Eq.1}$$

where D_i = Natural or regenerated OSL, initial 0.2 s
 L_i = Background natural or regenerated OSL, final 5 s
 d_i = Test dose OSL, initial 0.2 s
 x = Scaling factor, 0.08

The error on each signal parameter is based on counting statistics, reflected by the square-root of measured values. The propagation of these errors within Eq. 1 generating σS_i follows the general formula given in Eq. 2. σS_i were then used to define fitting and interpolation errors within exponential plus linear regressions.

For D_i values, systematic errors accommodate uncertainty in radionuclide conversion factors (5%), β attenuation coefficients (5%), matrix density (0.20 g.cm^{-3}), vertical thickness of sampled section (specific to sample collection device), saturation moisture content (3%), moisture content attenuation (2%) and burial moisture content (25% relative, unless direct evidence exists of the magnitude and period of differing content). Experimental errors are associated with radionuclide quantification for each sample by Ge gamma spectrometry.

The propagation of these errors through to age calculation was quantified using the expression,

$$\sigma y (\delta y / \delta x) = (\sum ((\delta y / \delta x_i) \cdot \sigma x_i)^2)^{1/2} \quad \text{Eq. 2}$$

where y is a value equivalent to that function comprising terms x_i , and where σy and σx_i are associated uncertainties.

Errors on age estimates are presented as combined systematic and experimental errors and experimental errors alone. The former (combined) error should be considered when comparing luminescence ages herein with independent chronometric controls. The latter assumes systematic errors are common to luminescence age estimates generated by means identical to those detailed herein and enable direct comparison with those estimates.

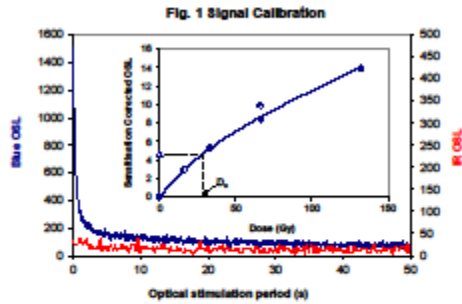


Fig. 1 Signal Calibration Natural blue and laboratory-induced infrared (IR) OSL signals. Detectable IR signal decays are diagnostic of feldspar contamination. Inset, the natural blue OSL signal (open triangle) of each aliquot is calibrated against known laboratory doses to yield equivalent dose (D_e) values. Results of low and high doses (open diamonds) illustrate the success of sensitivity correction.

Fig. 2 Dose Recovery The acquisition of D_e values is necessarily predicated upon thermal treatment of aliquots succeeding environmental and laboratory irradiation. The Dose Recovery test quantifies the combined effects of thermal transfer and sensitisation on the natural signal using a precise lab dose to simulate natural dose. Based on this an appropriate thermal treatment is selected to generate the final D_e value.

Fig. 3 Inter-aliquot D_e distribution Abernethy plot of inter-aliquot statistical concordance in D_e values derived from natural irradiation. Discordant data (those points lying beyond ±1 standardised in D_e) reflect heterogeneous dose absorption and/or inaccuracies in calibration.

Fig. 4 Signal Analysis Statistically significant increase in natural D_e value with signal stimulation period is indicative of a partially-bleached signal, provided a significant increase in D_e results from simulated partial bleaching followed by insignificant adjustment in D_e for simulated zero and full bleach conditions. Ages from such samples are considered maximum estimates. In the absence of a significant rise in D_e with stimulation time, simulated partial bleaching and successful bleach tests are not assessed.

Fig. 5 U Activity Statistical concordance (equilibrium) in the activities of the daughter radionuclide ²¹⁰Pb with its parent ²¹⁰Pu may signify the temporal stability of D_e estimates from these chains. Significant differences (dis-equilibrium; >20%) in activity indicate addition or removal of isotopes creating a time-dependent shift in D_e values and increased uncertainty in the accuracy of age estimates. A 20% disequilibrium marker is also shown.

Fig. 6 Age Range The Cumulative frequency plot indicates the inter-aliquot variability in age. It also shows the mean age range; an estimate of sediment burial period based on mean D_e and D₀ values with associated analytical uncertainties. The maximum influence of temporal variations in D_e forced by minima-maxima variation in moisture content and overburden thickness is outlined and may prove instructive where there is uncertainty in these parameters. However the combined extremes represented should not be construed as preferred age estimates.

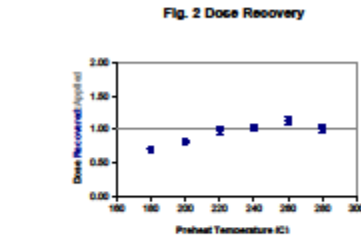
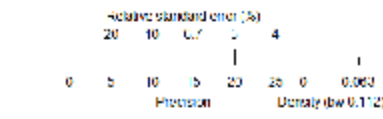
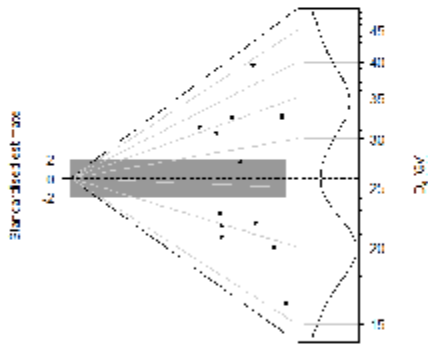


Fig. 3 Inter-aliquot D_e distribution



Sample: GL18006

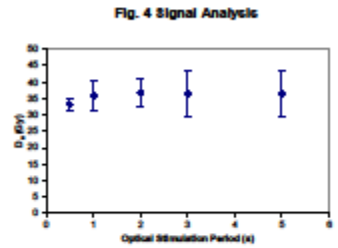


Fig. 5 U Decay Activity

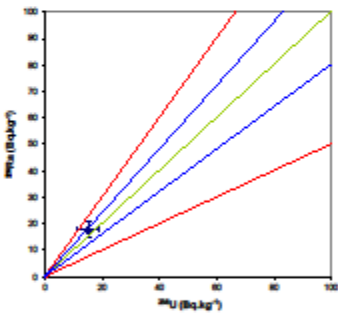
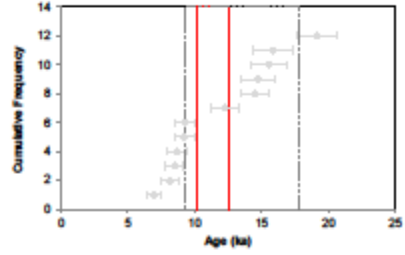


Fig. 6 Age Range



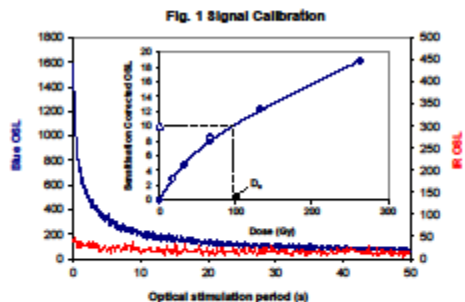


Fig. 1 Signal Calibration

Fig. 1 Signal Calibration Natural blue and laboratory-induced infrared (IR) OSL signals. Detectable IR signal decays are diagnostic of feldspar contamination. Inset, the natural blue OSL signal (open triangle) of each aliquot is calibrated against known laboratory doses to yield equivalent dose (D_0) values. Results of low and high doses (open diamonds) illustrate the success of sensitivity correction.

Fig. 2 Dose Recovery The acquisition of D_0 values is necessarily predicated upon thermal treatment of aliquots succeeding environmental and laboratory irradiation. The Dose Recovery test quantifies the combined effects of thermal transfer and sensitisation on the natural signal using a precise lab dose to simulate natural dose. Based on this an appropriate thermal treatment is selected to generate the final D_0 value.

Fig. 3 Inter-aliquot D_0 distribution Abernethy plot of inter-aliquot statistical concordance in D_0 values derived from natural irradiation. Discordant data (those points lying beyond ± 2 standardised D_0) reflect heterogeneous dose absorption and/or inaccuracies in calibration.

Fig. 4 Signal Analysis Statistically significant increase in natural D_0 value with signal stimulation period is indicative of a partially-bleached signal, provided a significant increase in D_0 results from simulated partial bleaching followed by insignificant adjustment in D_0 for simulated zero and full bleach conditions. Ages from such samples are considered maximum estimates. In the absence of a significant rise in D_0 with stimulation time, simulated partial bleaching and successful bleach tests are not assessed.

Fig. 5 U Activity Statistical concordance (equilibrium) in the activities of the daughter radionuclide ^{214}Pb with its parent ^{214}Po may signify the temporal stability of D_0 estimations from these chains. Significant differences (disequilibrium; $>20\%$) in activity indicate addition or removal of isotopes creating a time-dependent shift in D_0 values and increased uncertainty in the accuracy of age estimates. A 20% disequilibrium marker is also shown.

Fig. 6 Age Range The Cumulative frequency plot indicates the inter-aliquot variability in age. It also shows the mean age range; an estimate of sediment burial period based on mean D_0 and D_1 values with associated analytical uncertainties. The maximum influence of temporal variations in D_0 forced by minima-maxima variation in moisture content and overburden thickness is outlined and may prove instructive where there is uncertainty in these parameters. However the combined extremes represented should not be construed as preferred age estimates.

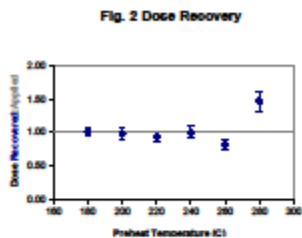
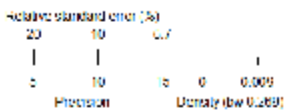
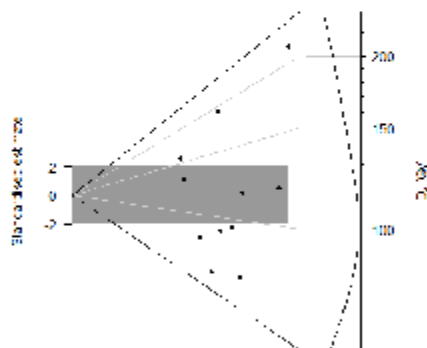


Fig. 2 Dose Recovery

Fig. 3 Inter-aliquot D_0 distribution



Sample: GL18007

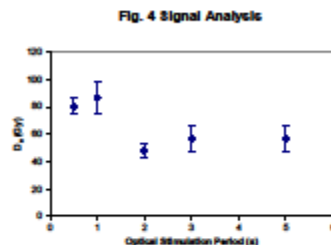


Fig. 4 Signal Analysis

Fig. 5 U Decay Activity

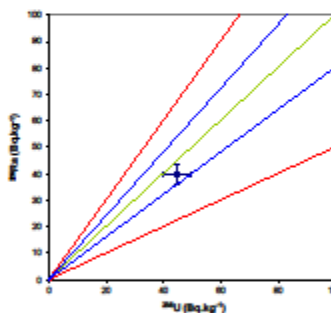
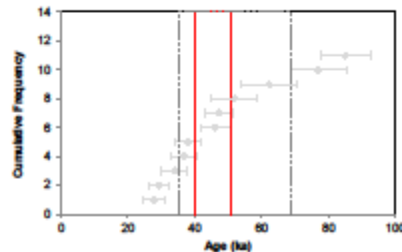


Fig. 6 Age Range



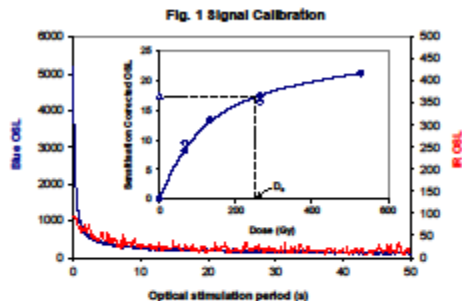


Fig. 1 Signal Calibration

Fig. 1 Signal Calibration Natural blue and laboratory-induced infrared (IR) OSL signals. Detectable IR signal decays are diagnostic of feldspar contamination. Inset, the natural blue OSL signal (open triangle) of each aliquot is calibrated against known laboratory doses to yield equivalent dose (D_e) values. Results of low and high doses (open diamonds) illustrate the success of sensitivity correction.

Fig. 2 Dose Recovery The acquisition of D_e values is necessarily predicated upon thermal treatment of aliquots succeeding environmental and laboratory irradiation. The Dose Recovery test quantifies the combined effects of thermal transfer and sensitisation on the natural signal using a precise lab dose to simulate natural dose. Based on this an appropriate thermal treatment is selected to generate the final D_e value.

Fig. 3 Inter-aliquot D_e distribution Abernethy plot of inter-aliquot statistical concordance in D_e values derived from natural irradiation. Discordant data (those points lying beyond ± 2 standardised D_e) reflect heterogeneous dose absorption and/or inaccuracies in calibration.

Fig. 4 Signal Analysis Statistically significant increase in natural D_e value with signal stimulation period is indicative of a partially-bleached signal, provided a significant increase in D_e results from simulated partial bleaching followed by insignificant adjustment in D_e for simulated zero and full bleach conditions. Ages from such samples are considered maximum estimates. In the absence of a significant rise in D_e with stimulation time, simulated partial bleaching and successful bleach tests are not assessed.

Fig. 5 U Activity Statistical concordance (equilibrium) in the activities of the daughter radionuclide ^{210}Pb with its parent ^{210}Po may signify the temporal stability of D_e estimates from these chains. Significant differences (dis-equilibrium; $>20\%$) in activity indicate addition or removal of isotopes creating a time-dependent shift in D_e values and increased uncertainty in the accuracy of age estimates. A 20% disequilibrium marker is also shown.

Fig. 6 Age Range The Cumulative frequency plot indicates the inter-aliquot variability in age. It also shows the mean age range; an estimate of sediment burial period based on mean D_e and D_e values with associated analytical uncertainties. The maximum influence of temporal variations in D_e forced by minima-maxima variation in moisture content and overburden thickness is outlined and may prove instructive where there is uncertainty in these parameters. However the combined extremes represented should not be construed as preferred age estimates.

Fig. 2 Dose Recovery

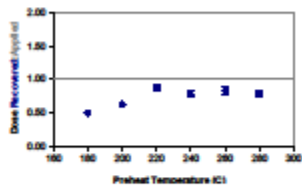
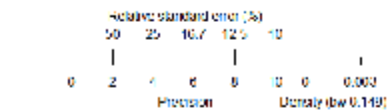
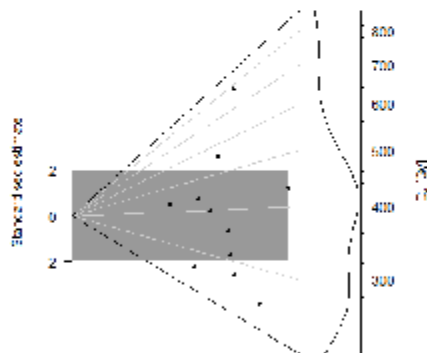


Fig. 3 Inter-aliquot D_e distribution



Sample: GL18008

Fig. 4 Signal Analysis

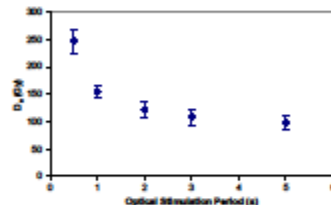


Fig. 5 U Decay Activity

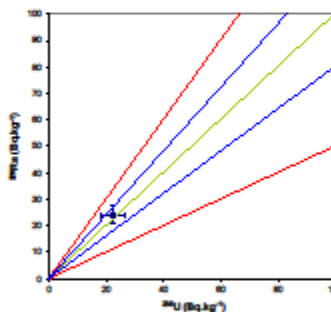
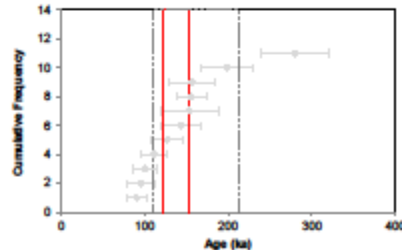


Fig. 6 Age Range



References

- Adamiec, G. and Aitken, M.J. (1998) Dose-rate conversion factors: new data. *Ancient TL*, 16, 37-50.
- Agersnap-Larsen, N., Bulur, E., Bøtter-Jensen, L. and McKeever, S.W.S. (2000) Use of the LM-OSL technique for the detection of partial bleaching in quartz. *Radiation Measurements*, 32, 419-425.
- Aitken, M. J. (1998) *An introduction to optical dating: the dating of Quaternary sediments by the use of photon-stimulated luminescence*. Oxford University Press.
- Bailey, R.M., Singarayer, J.S., Ward, S. and Stokes, S. (2003) Identification of partial resetting using D_e as a function of illumination time. *Radiation Measurements*, 37, 511-518.
- Bateman, M.D., Frederick, C.D., Jaiswal, M.K., Singhvi, A.K. (2003) Investigations into the potential effects of pedoturbation on luminescence dating. *Quaternary Science Reviews*, 22, 1169-1176.
- Bateman, M.D., Boulter, C.H., Carr, A.S., Frederick, C.D., Peter, D. and Wilder, M. (2007) Detecting post-depositional sediment disturbance in sandy deposits using optical luminescence. *Quaternary Geochronology*, 2, 57-64.
- Berger, G.W. (2003). Luminescence chronology of late Pleistocene loess-paleosol and tephra sequences near Fairbanks, Alaska. *Quaternary Research*, 60, 70-83.
- Bøtter-Jensen, L., Mejdahl, V. and Murray, A.S. (1999) New light on OSL. *Quaternary Science Reviews*, 18, 303-310.
- Bøtter-Jensen, L., McKeever, S.W.S. and Wintle, A.G. (2003) *Optically Stimulated Luminescence Dosimetry*. Elsevier, Amsterdam.
- Dietze, M., Kreutzer, S., Burow, C., Fuchs, M.C., Fischer, M., Schmidt, C. (2016) The abanico plot: visualising chronometric data with individual standard errors. *Quaternary Geochronology*, 31, 1-7.
- Duller, G.A.T (2003) Distinguishing quartz and feldspar in single grain luminescence measurements. *Radiation Measurements*, 37, 161-165.
- Galbraith, R. F., Roberts, R. G., Laslett, G. M., Yoshida, H. and Olley, J. M. (1999) Optical dating of single and multiple grains of quartz from Jinmium rock shelter (northern Australia): Part I, Experimental design and statistical models. *Archaeometry*, 41, 339-364.
- Gliganic, L.A., May, J.-H. and Cohen, T.J. (2015). All mixed up: using single-grain equivalent dose distributions to identify phases of pedogenic mixing on a dryland alluvial fan. *Quaternary International*, 362, 23-33.
- Gliganic, L.A., Cohen, T.J., Slack, M. and Feathers, J.K. (2016) Sediment mixing in Aeolian sandsheets identified and quantified using single-grain optically stimulated luminescence. *Quaternary Geochronology*, 32, 53-66.
- Huntley, D.J., Godfrey-Smith, D.I. and Thewalt, M.L.W. (1985) Optical dating of sediments. *Nature*, 313, 105-107.
- Hubbell, J.H. (1982) Photon mass attenuation and energy-absorption coefficients from 1keV to 20MeV. *International Journal of Applied Radioisotopes*, 33, 1269-1290.

- Hütt, G., Jaek, I. and Tchonka, J. (1988) Optical dating: K-feldspars optical response stimulation spectra. *Quaternary Science Reviews*, 7, 381-386.
- Jacobs, A., Wintle, A.G., Duller, G.A.T, Roberts, R.G. and Wadley, L. (2008) New ages for the post-Howiesons Poort, late and finale middle stone age at Sibdu, South Africa. *Journal of Archaeological Science*, 35, 1790-1807.
- Lombard, M., Wadley, L., Jacobs, Z., Mohapi, M. and Roberts, R.G. (2011) Still Bay and serrated points from the Umhlatuzana rock shelter, Kwazulu-Natal, South Africa. *Journal of Archaeological Science*, 37, 1773-1784.
- Markey, B.G., Bøtter-Jensen, L., and Duller, G.A.T. (1997) A new flexible system for measuring thermally and optically stimulated luminescence. *Radiation Measurements*, 27, 83-89.
- Mejdahl, V. (1979) Thermoluminescence dating: beta-dose attenuation in quartz grains. *Archaeometry*, 21, 61-72.
- Murray, A.S. and Olley, J.M. (2002) Precision and accuracy in the Optically Stimulated Luminescence dating of sedimentary quartz: a status review. *Geochronometria*, 21, 1-16.
- Murray, A.S. and Wintle, A.G. (2000) Luminescence dating of quartz using an improved single-aliquot regenerative-dose protocol. *Radiation Measurements*, 32, 57-73.
- Murray, A.S. and Wintle, A.G. (2003) The single aliquot regenerative dose protocol: potential for improvements in reliability. *Radiation Measurements*, 37, 377-381.
- Murray, A.S., Olley, J.M. and Caitcheon, G.G. (1995) Measurement of equivalent doses in quartz from contemporary water-lain sediments using optically stimulated luminescence. *Quaternary Science Reviews*, 14, 365-371.
- Olley, J.M., Murray, A.S. and Roberts, R.G. (1996) The effects of disequilibria in the Uranium and Thorium decay chains on burial dose rates in fluvial sediments. *Quaternary Science Reviews*, 15, 751-760.
- Olley, J.M., Caitcheon, G.G. and Murray, A.S. (1998) The distribution of apparent dose as determined by optically stimulated luminescence in small aliquots of fluvial quartz: implications for dating young sediments. *Quaternary Science Reviews*, 17, 1033-1040.
- Olley, J.M., Caitcheon, G.G. and Roberts R.G. (1999) The origin of dose distributions in fluvial sediments, and the prospect of dating single grains from fluvial deposits using -optically stimulated luminescence. *Radiation Measurements*, 30, 207-217.
- Olley, J.M., Pietsch, T. and Roberts, R.G. (2004) Optical dating of Holocene sediments from a variety of geomorphic settings using single grains of quartz. *Geomorphology*, 60, 337-358.
- Pawley, S.M., Toms, P.S., Armitage, S.J., Rose, J. (2010) Quartz luminescence dating of Anglian Stage fluvial sediments: Comparison of SAR age estimates to the terrace chronology of the Middle Thames valley, UK. *Quaternary Geochronology*, 5, 569-582.
- Prescott, J.R. and Hutton, J.T. (1994) Cosmic ray contributions to dose rates for luminescence and ESR dating: large depths and long-term time variations. *Radiation Measurements*, 23, 497-500.

Singhvi, A.K., Bluszcz, A., Bateman, M.D., Someshwar Rao, M. (2001). Luminescence dating of loess-palaeosol sequences and coversands: methodological aspects and palaeoclimatic implications. *Earth Science Reviews*, 54, 193-211.

Smith, B.W., Rhodes, E.J., Stokes, S., Spooner, N.A. (1990) The optical dating of sediments using quartz. *Radiation Protection Dosimetry*, 34, 75-78.

Spooner, N.A. (1993) The validity of optical dating based on feldspar. Unpublished D.Phil. thesis, Oxford University.

Templer, R.H. (1985) The removal of anomalous fading in zircons. *Nuclear Tracks and Radiation Measurements*, 10, 531-537.

Wallinga, J. (2002) Optically stimulated luminescence dating of fluvial deposits: a review. *Boreas* 31, 303-322.

Wintle, A.G. (1973) Anomalous fading of thermoluminescence in mineral samples. *Nature*, 245, 143-144.

Zimmerman, D. W. (1971) Thermoluminescent dating using fine grains from pottery. *Archaeometry*, 13, 29-52.